



# anti-aging

weekly

No: 4

Telomer Bütünlüğünün Korunması  
Sağlıklı Bir Yaşam ve Yaşlanma  
İçin Önemlidir

 anti-aging.com.tr



Değerli Hekimlerimiz,

Bu sayımızda telomer uzunluğunun sağlıklı ve uzun yaşam üzerine etkilerini gösteren ve saygın dergilerde yayınlanmış 2 makale ile yeniden karşınızdayız. Bu iki makale hakkında meslektaşınız Sayın Doç. Dr. Şehime G. TEMEL'in her iki makale hakkındaki değerli yorumlarını bir sonraki sayfada bulabilirsiniz.

Sizlere telomer biyolojisinin kısaca gelişim aşamalarını, yine Michael Fossel MD'nin Telomerase Revolution adlı kitabından yararlanarak aktarmak istiyorum.

1665 yılında Robert Hooke organizmaların hücrelerden oluştuğunu keşfetmişti.

1889'de endokrinoloji alanında öncülerden Charles Edouard Brown Sequard, hayvan testislerinden (guinea domuzu, köpek ve maymunlardan) elde ettiği bazı ekstraktların insanları gençleştirdiğini ve yaşamlarını uzattığı iddia etmişti.

1934'de ise Cornell Üniversitesi'nden Mary Crowell ve Clive McCay farelerde ileri düzeyde kalori kısıtlaması sayesinde yaşam sürelerini iki katına çıkarabildiklerini ileri sürdüler. Ancak bugüne dek insanlarda veya primatlarda bu durum kesin olarak tekrar edilemedi.

1938'de Hermann Müller, Drosophila melanogaster isimli meyve sineğini incelerken telomerleri tanımlayan ilk bilim insanı oldu.

1940'da ise Barbara McClintock telomerlerin koruyucu görevlerini tarif etmiş ve daha sonra Nobel ödülü kazanmıştır.

1961'de Dr. Leonard Hayflick, insan hücrelerinin laboratuvar koşullarında sadece 50-60 kez bölünme kapasitesinin olduğunu ve daha sonra programlı ölüm safhasına geçtiğini keşfetti. İnsan ömrünün 125 yıl ile sınırlı olduğu gerçeğini tanımlanması ile Hayflick Limiti denen bu durum tıp literatüründe yerini aldı. Ancak Dr. Hayflick bu durumun sebebini bulamamıştı.

1971'de Rus bilim adamı Alexey Olovnikov, Hayflick Limitinin telomerlerin kısalması nedeni ile olabileceğine dair bir bilimsel makale yayınladı.

1972 yılında ise Denham Harmon yaşlanmada mitokondrideki serbest radikal hasarına dair bir yayın yapmıştı.

1990 yılında Dr. Mike West isimli girişimci bir hekim Geron isimli biyoteknoloji firmasını kurdu. Temel amacı yaşlanmayı tedavi etmek ile ilgili bir çözüm geliştirmekti ve bunun için telomer biyolojisinin işe yarayabileceğini öngörmekteydi.

1993 yılında ise Calvin Harley ve arkadaşları progeria adı verilen ve çocukların 10'lu yaşlarda ileri yaşlılık belirtileri nedeni ile kaybedildiği hastalığın temelinde hızlı telomer kısalması olduğunu keşfetti.

1998 yılında Michael Fossel telomer kısalmasının engellenmesi ile yaşlılığın engellenebileceğine dair ilk bilimsel makalesini yayınladı.

1999 yılında Geron'daki bilim insanları telomer boyunun kısalmasının hücre yaşlanmasının bir sonucu değil tam tersine hücre yaşlanmasının doğrudan sebebi olduğunu ispatladılar. Hatta telomer boyunun uzatılması hücredeki yaşlanma işaretlerini sıfırlamakta, hücresel biyolojik saati geri almaktaydı.

2000 yılında Geron, astragalus adlı bitkinin kökünden elde ettiği tek bir izole molekül ile telomerleri uzattığını ispat ettiği TA-65 molekülünün patentini aldı. Aynı yıl Rita Effros, UCLA üniversitesinde bu molekülün bağışıklık sistemi üzerindeki gençleştirici etkileri hakkında klinik çalışma başlattı.

2002 yılında Geron daha çok kanser tedavisinde kullanılabilecek bir molekül üzerinde çalışmak üzere TA-65 projesini tamamen TA Sciences isimli firmaya sattı. Geron kanser üzerinde etki gösteren bir telomerase baskılayıcı ile molekülü keşfetmiş olup bugünlerde molekül halen test aşamasındadır.

2007 yılında ise TA Sciences, TA-65 isimli besin desteğini geliştirerek kullanıma sundu ve insanlar üzerindeki klinik çalışmalara başladı.

2009'da Dr. Elizabeth Blackburn, Dr. Carol Greider ve Dr. Jack Szotak, telomer boyunun telomeraz adı verilen bir enzim sayesinde yönetildiğini bulmaları nedeni ile Nobel Ödülü'ne layık görüldüler.

2010 yılında telomer boyunun ölçümünü gerçekleştiren Life Length isimli laboratuvar telomer biyolojisinin önemli isimlerinden Dr. Maria Blasco tarafından Madrid / İspanya'da kuruldu.

2011'de ilk kez bir memelinin yaşlanmasının, telomer boyunun uzatılması sayesinde geri çevrilebileceği gösterildi. Harvard Üniversite'sinden Dr. DePinho ve ekibi tarafından yayınlanan makale bilim dünyasında saygın bir dergi olan Nature'da yer aldı (2. sayımızda sizler ile paylaşmıştık).

2012 yılında Maria Blasco, hayvanlarda telomerin restore edilmesi ile birçok yaşlılığa bağlı hastalığın geri dönüştürülebildiğini ispatladı.

2016 yılına geldiğimizde telomer ve telomeraz konusunda yayınlanmış yaklaşık 20.000 makale bulunmakta ve bu sayı giderek artmaktadır.

Bu gelişimden de göreceğiniz gibi telomer biyolojisi önümüzdeki yıllarda önemi daha da artmaya aday bir konudur. Özellikle anti-aging alanında telomer biyolojisi çok önemli bir potansiyel vaat etmektedir.

Bir sonraki sayımıza dek telomerlerinizin hep uzun kalması dileği ile...

  
Kubilay Türkmen

Bizi sosyal medyada takip edebilirsiniz.



TA65tr



Instagram TA65tr



TA65tr

Değerli meslektaşlarım;

Hepimizin bildiği üzere telomerler; kromozomların kararlılığı ve hücre yaşamı için gerekli olan özelleşmiş heterokromatin yapılarıdır.

Ekteki 1.makale saygın ve prestijli bilim dergilerinden Cell'de 1999 yılında yayımlanmıştır.

Telomer biyolojisine katkı sağlayan bu çalışmada hipotez telomerazları etkisizleştirilen farelerde yaşlılığın patofizyolojik sonuçlarının gözlenmesidir. Çalışmada; telomerazları etkisizleştirilmiş farelerin telomer fonksiyonunun kaybı ile yaşlanmaya ait tüm patofizyolojik belirtiler gözlenmemiş ise de; yaşa bağlı telomer kısalması ve beraberindeki genetik kararsızlığı; kısalmış ömrün yanı sıra, yara iyileşmesinin gecikmesi, ülseratif deri lezyonlarının artması, erkek fertilitésinin azalması veya infertil olması, saç dökülmesi, saç beyazlaşmasının hızlanması ve hematopoetik hücrelerin rezervelerinin azalması gibi etkileri de beraberinde getirdiği gözlenmiştir. Bunun yanı sıra bu farelerde spontan olarak gelişen kanser türlerinde ve insidansında artış olduğu da gösterilmiştir. Çalışmada telomerleri etkisizleştirilmiş farelerin özellikle birçok fizyolojik stres durumuna cevap verme yeteneklerinin farelerin artan yaşlarıyla birlikte azaldığı görülmüştür. Dolayısıyla bu çalışma ile telomer uzunluğu kararlılığının; sağlıklı ve iyi yaşlanma için çok önemli bir gösterge olduğu ispatlanmıştır.

Ekteki diğer makale ise hematolojik hastalıklarla ilgili saygın bilim dergilerinden Blood'da 5 Nisan'da yayımlanmıştır. Telomer biyolojisine katkı sağlayan bu çalışmadaki hipotez ise aplastik anemili farelerde oluşan telomeraz ve/veya ilgili genlerdeki mutasyonun düzeltilmesi ile bulguların geri dönüp dönmeyeceğinin gözlenmesidir.

Hepimizin yakından bildiği üzere aplastik anemi periferal pansitopeni ve kemik iliği hipoplazisi ile seyreden öldürücü bir kemik iliği hastalığıdır. Bu hastalık kalıtılmış veya kazanılmış olarak hayatın herhangi bir döneminde ortaya çıkabilir. Kalıtılmış grubun bir alt grubunda hematopoetik kök ve öncü hücrelerde telomeraz ve/veya telomer ile ilişkili diğer genlerde mutasyonların olması sonucu çok kısalmış telomerler görülür. Kazanılmış aplastik anemilerde ise telomer kısalması kemik iliği kök ve öncü hücrelerinin hızlanmış siklusuna sekonder olarak görülmektedir.

Yapılan bu çalışmada araştırmacılar; telomeraz aktivitesinin tedavi edici etkisini telomeraz Tert genini taşıyan adeno ile ilişkili virus (AAV) 9 gen terapi vektörünü kullanarak iki farklı bağımsız fare hattında test etmişlerdir.

Yüksek doz AAV9-Tert tedavisinin hematopoetik kök ve öncü hücreleri uyararak kemik iliğinde aplastik anemiyi kurtardığı ve fare yaşamının sürmesini sağladığı görülürken boş vektör verilen farelerde bu olaylar gözlenmemiştir. Sağkalımın sağlanması telomer uzunluğunda görülen belirgin artış olarak değerlendirilmiştir.

Sonuç olarak araştırmacılar bu çalışmada telomeraz gen terapisi ile aplastik anemili farelerde telomer uzunluğu artışı sağlayarak aplastik anemili farelerin sağ kalımını sağlamıştır.

Bu iki makaleden de açık ve net bir şekilde görüldüğü üzere 'telomer bütünlüğünün korunması' sağlıklı bir yaşam ve yaşlanma için olmazsa olmaz unsurlardan birisidir. Bu yüzden değerli meslektaşlarımın hücresel ve doku bazlı anti-aging tedavi yaklaşımlarının yanı sıra genetik bazlı anti-aging yaklaşımlarına da yeni bir bakış açısı getirebileceğini düşündüğüm bu iki yayından faydalanabilmelerini dilerim.

Saygılarımla

Doç. Dr. Şehime G. TEMEL

*Tıp Doktoru*

*Histoloji ve Embriyoloji Bilim Doktoru*

*İnsan Genetiği Bilimi Araştırmacısı*

# Longevity, Stress Response, and Cancer in Aging Telomerase-Deficient Mice

Karl Lenhard Rudolph,<sup>1</sup> Sandy Chang,<sup>3</sup>  
Han-Woong Lee,<sup>6</sup> Maria Blasco,<sup>7</sup>  
Geoffrey J. Gottlieb,<sup>4</sup> Carol Greider,<sup>5</sup>  
and Ronald A. DePinho<sup>1,2,8</sup>

<sup>1</sup>Department of Adult Oncology  
Dana Farber Cancer Institute  
44 Binney Street, M413  
Boston, Massachusetts 02115

<sup>2</sup>Department of Medicine and Genetics

<sup>3</sup>Department of Pathology and  
Brigham and Women's Hospital  
Harvard Medical School  
Boston, Massachusetts 02110

<sup>4</sup>Quest Diagnostics Inc.

Anatomical Pathology  
Teterboro, New Jersey 07608

<sup>5</sup>Department of Molecular Biology and Genetics  
Johns Hopkins University School of Medicine  
Baltimore, Maryland 21205

<sup>6</sup>Center of Molecular Medicine  
Samsung Biomedical Research Institute  
Sungkyunkwan University School of Medicine  
Seoul 135-230  
Korea

<sup>7</sup>Department of Immunology and Oncology  
National Centre of Biotechnology  
Madrid E-28049  
Spain

## Summary

Telomere maintenance is thought to play a role in signaling cellular senescence; however, a link with organismal aging processes has not been established. The telomerase null mouse provides an opportunity to understand the effects associated with critical telomere shortening at the organismal level. We studied a variety of physiological processes in an aging cohort of *mTR*<sup>-/-</sup> mice. Loss of telomere function did not elicit a full spectrum of classical pathophysiological symptoms of aging. However, age-dependent telomere shortening and accompanying genetic instability were associated with shortened life span as well as a reduced capacity to respond to stresses such as wound healing and hematopoietic ablation. In addition, we found an increased incidence of spontaneous malignancies. These findings demonstrate a critical role for telomere length in the overall fitness, reserve, and well being of the aging organism.

## Introduction

Telomeres are essential for chromosomal stability and cell viability in a variety of different species (Greider,

1996). In primary human cells, telomeres shorten with passage in culture, and progressive telomere shortening ultimately limits the replicative capacity of cultured cells (Harley et al., 1990; Allsopp et al., 1992; Wright and Shay, 1992; Counter, 1996; de Lange, 1998). It has been suggested that telomere-associated cellular senescence may contribute to certain age-related disorders, including an increase in cancer incidence, wrinkling and diminished skin elasticity, atherosclerosis, osteoporosis, weight loss, and others (Salk, 1982). Although aged organ systems function adequately to maintain baseline health, short telomeres could be linked more directly to a fundamental feature of aging: a reduced capacity to respond to acute and chronic illness.

Many diverse genes, such as those involved in gene silencing, DNA repair, genomic stability, and growth factor signaling, have emerged as strong determinants of life span in a variety of species (Dorman et al., 1995; Guarente, 1996; Wright et al., 1996; Smeal and Guarente, 1997). Less clear, however, is the relevance of progressive telomere shortening as a potential factor in organismal aging (Johnson et al., 1998). In *Saccharomyces cerevisiae*, although telomere shortening in EST1 mutants causes rapid loss of cell viability (Lundblad and Szostak, 1989), telomere length holds constant over the life span of normal cells, implying that telomere shortening is not a cause of aging in yeast (D'Mello and Jazwinski, 1991; Austriaco and Guarente, 1997; Sinclair et al., 1998). In contrast, the tight relationship between replicative senescence and telomere shortening in cultured human cells has led to the view that telomere length regulation may provide a molecular explanation for diminished reserve and cellular senescence in aged tissues (Cooke and Smith, 1986; Harley et al., 1990; Hastie et al., 1990; Lindsey et al., 1991; Allsopp et al., 1992; Vaziri et al., 1994; Harley, 1997; Frenck et al., 1998). Age-dependent telomere loss may contribute to a reduction in viable cells, altered differentiation functions, and impaired regenerative/proliferative responses, particularly in the settings of stress such as those seen in chronic infections, cirrhosis, chronic skin ulcerations, hypertensive vascular injury, among others (Chang and Harley, 1995; Kitada et al., 1995; Effros et al., 1996). One might anticipate that high turnover organs such as the skin, lymphoid, and gastrointestinal tract would be more adversely affected due to an accelerated loss of telomere repeats (Campisi, 1998).

In humans, telomeres are short, and telomerase activity is low or undetectable in many somatic tissues but present in germ cells, activated leukocytes, and stem cells from a variety of organs (Harley et al., 1994; Wright et al., 1996; Newbold, 1997). However, the degree to which telomerase maintains telomeres in these tissues during aging has not yet been fully explored. The laboratory mouse, an inbred strain of *Mus musculus*, possesses much longer telomeres, and telomerase activity and gene expression of the catalytic subunit of telomerase (TERT) appear to be less stringently regulated in somatic cells (Kipling and Cooke, 1990; Prowse et al., 1993; Prowse and Greider, 1995; Zijlmans et al., 1997;

<sup>8</sup>To whom correspondence should be addressed (e-mail: ron\_depinho@dfci.harvard.edu).

Greenberg et al., 1998). Although the mouse is a good model for studying telomerase activity and its regulation, the long telomeres in this species, despite modest attrition with aging (K. L. R. and R. A. D., unpublished data), make it unlikely that telomere length plays a prominent role in normal mouse aging.

A critical evaluation of the effect of telomere shortening on aging *in vivo* has been hampered by the lack of mammalian-based model systems. We have previously generated telomerase-deficient mice through disruption of the gene encoding the essential RNA component of the telomerase holoenzyme (mTR) (Blasco et al., 1997). These studies established that mTR<sup>-/-</sup> mice exhibit progressive telomere shortening with each successive generation arising from mTR<sup>-/-</sup> intercrosses (Blasco et al., 1997; Lee et al. 1998). Sixth generation mice (G6) were infertile, had a decreased proliferative capacity of splenocytes and bone marrow cells *in vivo*, and had an increased embryonic lethality due to neural tube closure defects (Lee et al., 1998; Herrera et al., 1999). Third generation mTR<sup>-/-</sup> mice (G3) possess shortened telomeres early in life but, at this point, appear to be phenotypically normal in every respect (Lee et al., 1998). The current study focused primarily on the physiological consequences in an aging population of G3 mice and compared these results to first and sixth generation mTR<sup>-/-</sup> mice (G1 and G6, respectively) to dissect the contribution of telomere dysfunction to the pathophysiological processes and events associated with aging.

## Results

To assess the effect of progressive telomere loss on mice with increased age, we studied a cohort of mice over a 2.5 year period. Specifically, 63 mTR<sup>+/+</sup>, 35 mTR<sup>-/-</sup> G1, 35 mTR<sup>-/-</sup> G3, and 36 mTR<sup>-/-</sup> G6 mice were analyzed for a broad spectrum of phenotypes associated with the aging process. For brevity, we refer to successive generations of telomerase-deficient mice as G1 (for G1 mTR<sup>-/-</sup>), G2 (for G2 mTR<sup>-/-</sup>), and so on.

### Hair Graying, Alopecia, and Skin Lesions

A dramatic increase in the incidence of hair graying and alopecia (hair loss) was noted in aging G3 and G6 mice compared to age-matched mTR<sup>+/+</sup> mice (Figures 1A–1D: 25% in mTR<sup>+/+</sup>, 54% in G3, and 60% in G6, in animals older than 15 months). In addition, hair graying was seen at younger ages: some of the G6 animals showed graying at 6 months of age, while none of the G3 or mTR<sup>+/+</sup> mice showed alopecia or hair graying at this age. Hair growth is a cyclic process in which the hair follicle progresses through an active growth phase (anagen), an involuting phase (catagen), and a resting phase (telogen) (Courtois et al., 1995). Dorsal skin specimens from 15- to 18-month-old G3 and G6 mice showed equal numbers of hair follicles in the dermis compared to mTR<sup>+/+</sup> animals (Figures 1E and 1F), but there was a clear increase in miniaturized, involuted, melanin-rich follicles in the superficial dermis (Figure 1F). The number of hair follicles in the growth phase (anagen) relative to the resting phase was 2- to 3-fold lower in G3 and G6 compared to mTR<sup>+/+</sup> animals (Figures 1E and 1F). These

histopathological findings in the aged balding G3 and G6 mice are consistent with a diagnosis of androgenetic alopecia (male pattern baldness; Courtois et al., 1994). In addition to changes in hair number and color, a higher incidence of severe ulcerative skin lesions were seen in G3 and G6 mice 15 months and older compared to mTR<sup>+/+</sup> animals (Figures 1D, 1G, and 1H). While the frequency of skin lesions in G3 and G6 animals is similar, the onset of skin ulcerations was earlier in life in G6 compared to mTR<sup>+/+</sup> and G3 animals (average age: 25 months in mTR<sup>+/+</sup>, 26 months in G3, and 15 months in G6). These lesions were located predominantly at anatomical sites that are exposed to chronic mechanical stress, including distal limbs, perineum, snout, and throat area. Histologically, the skin lesions appeared as ulcerations with epidermal hyperplasia, hyperkeratosis, and underlying dermal fibrosis (Figure 1I). Such lesions are similar to those seen after chronic superficial trauma, particularly in debilitated elderly humans.

### Telomere Length Correlates Inversely to the Incidence of Skin Lesion, Alopecia, and Hair Graying

To determine whether telomere shortening played a causal role in the skin phenotypes described above, telomere length analysis was performed on G3 mice of different ages. Quantitative (Q)-FISH is a powerful method to determine telomere length in mice. Using this method, it was shown that telomere length decreases at a rate of 4–5 kb/generation in mTR null mice (Blasco et al., 1997). A newly developed flow cytometry fluorescence *in situ* hybridization (flow-FISH) method (Hultdin et al., 1998; Rufer et al., 1998) yielded very similar measurements of relative telomere length in successive mTR null MEF cultures (Figure 2A; Greenberg and R. A. D., unpublished data) and showed comparable results for different cell types within a given generation of mTR<sup>-/-</sup> mice (MEFs and peripheral blood leukocytes, data not shown). Flow-FISH allows the determination of telomere length in a large number of samples and can be performed on primary cells derived from peripheral bleeds. Since young G3 mice are phenotypically normal but progressively experience age-dependent compromise in the skin, flow-FISH telomere length determinations were obtained in leukocytes derived from multiple 1-month-old and >16-month-old G3 mice. A >50% reduction in telomere length was observed in old G3 samples relative to young G3 samples (Figure 2B,  $p = 0.035$ ), a finding consistent with the view that cell proliferation-dependent telomere erosion takes place in highly proliferative organ systems during life.

Next, we addressed whether differences in telomere length correlate with the presence or absence of age-associated cutaneous phenotypes in aged G3 mice. The relative telomere fluorescence signal of disease-free G3 mice was approximately 3-fold higher than in age-matched G3 mice afflicted with ulcerative skin lesions, hair graying, and alopecia (Figure 2C; comparing six animals with ulcerative skin lesions/hair graying or alopecia to five age-matched, disease-free animals,  $p = 0.029$ ). These data suggest that animals with shorter telomeres are more likely to display a disease phenotype

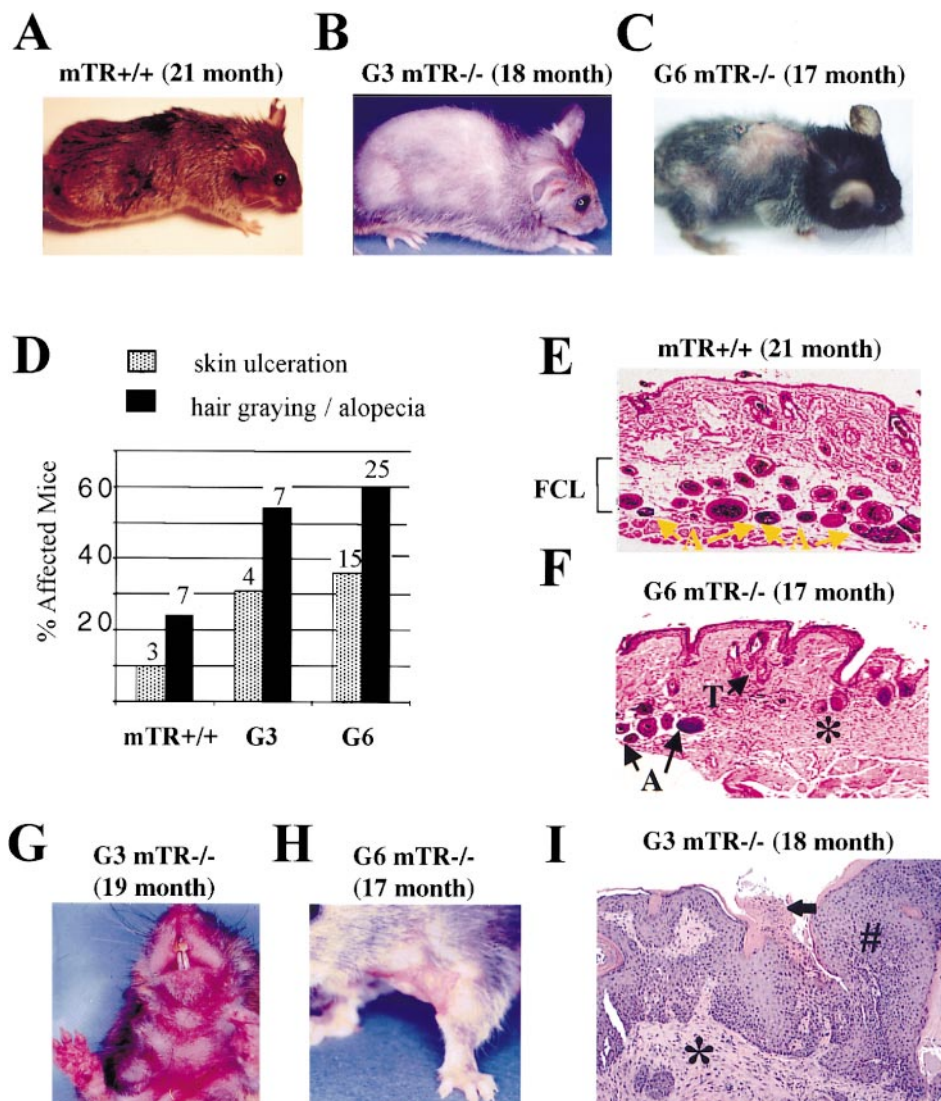


Figure 1. Increased Incidence of Skin Lesions, Alopecia, and Hair Graying in Aging mTR<sup>-/-</sup> Mice

(A–C) Representative examples of alopecia and hair graying in mTR<sup>+/+</sup> and mTR<sup>-/-</sup> mice.

(D) Incidence of ulcerative skin lesions and hair graying/alopecia in aged mTR<sup>+/+</sup>, G3, and G6 mice.

(E and F) Histologic appearance of representative H&E-stained skin sections from a 21-month-old mTR<sup>+/+</sup> mouse and a 17-month-old G6 mouse. Compared to the mTR<sup>+/+</sup> skin, in which nearly all hair follicles are in anagen (A, arrow), the G6 skin exhibited an increased frequency of hair follicles in telogen (T, arrows). In G6 skin, the subcutaneous fat cell layer (FCL) was replaced by dense, fibrous tissue (asterisk; 10× objective).

(G–H). Perioral, neck, and hind limb ulcerative skin lesions in G3 and G6 mice.

(I) H&E-stained section of an area of chronic injury in the vicinity of an ulcerative skin lesion in an 18-month-old G3 mouse (40× objective) showing marked epidermal hyperplasia (#), hyperkeratosis (arrow), and a dense dermal fibrosis (\*).

in the skin, further suggesting that telomere shortening in vivo contributes to disease susceptibility.

#### Telomere Shortening Does Not Cause Generalized Premature Aging

To determine whether other phenotypes often associated with aging occur early in the aging G3 animals, we carried out a broad histological survey of many organ systems (see Table 1). Analysis of the cardiovascular system, liver, kidneys, and brain showed no pathological changes typical of aging organisms (data not shown). A comprehensive serum chemistry profile that surveys

the functional metabolic and structural integrity of many organ systems was also normal (data not shown). Moreover, radiographic and histologic analyses of the femur failed to demonstrate osteoporosis, histological examination of aged arterial walls did not reveal signs of arteriosclerosis, and cataract formation occurred at similar frequencies in all groups (data not shown). Normal blood glucose levels after fasting and in response to glucose challenge showed that glucose tolerance was normal in these mice (data not shown). With the exception of modest reduction in spleen size, telomere shortening did not result in significant defects in the cellularity and

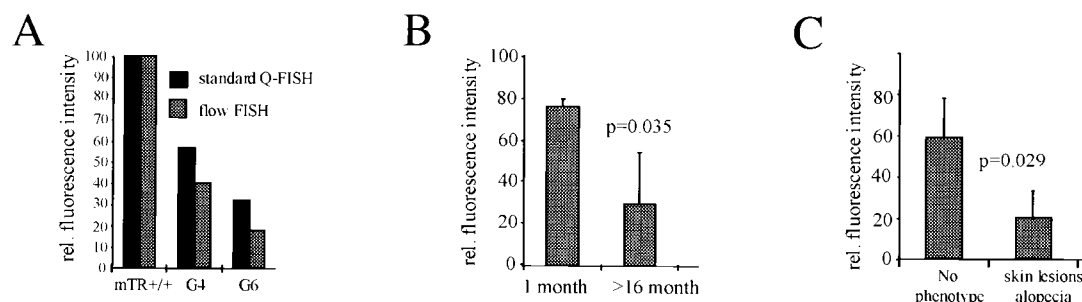


Figure 2. Telomere Length Decreases with Increasing Age and Correlates with the Skin Phenotype

(A) Relative telomere length of mouse embryo fibroblasts (MEF) derived from mTR<sup>+/+</sup>, G4, and G6 mice, comparing data obtained by flow-FISH and Q-FISH analysis (Greenberg and R. A. D., unpublished data). Fluorescence intensities of mTR<sup>+/+</sup> cells were set at 100%, and the relative intensity of G4 and G6 cells was calculated.

(B) Relative telomere length of peripheral WBC of 1-month-old and >16-month-old G3 mice.

(C) Relative telomere length of age-matched (15- to 24-month-old) G3 animals with and without skin lesions, alopecia, and hair graying.

architecture of hematopoietic organs or in the peripheral blood counts (data not shown). Thus, while telomere shortening with age directly affected the skin, mTR<sup>-/-</sup> mice did not display other phenotypes classically associated with aging.

### Reduced Longevity

Telomeres shorten during the lifetime of aging humans, but there is no direct correlation between the telomere length and the life span of different species (e.g., between mouse and humans) or within species of mice (reviewed in Greider, 1996). Thus, it is not yet clear to what extent telomere shortening might influence aging and longevity of complex organisms. There was no significant difference in the survival of G1 and G3 animals compared to mTR<sup>+/+</sup> controls (Figure 3). In contrast, a 15% increase in the incidence of spontaneous death was observed in 3- to 12-month-old G4–G6 animals. Further, at older ages, G6 mice showed elevated mortality. The survival curves of >12-month-old G4 and G5 animals paralleled those of mTR<sup>+/+</sup> and G1–G3 animals, while G6 mice died earlier. The 50% mortality mark occurred at 18 months for G6 mice, while 50% mortality was not reached until 24 months for mTR<sup>+/+</sup> and G1–G4 mice. As is often the case in natural death in humans, macroscopic and histological analyses at autopsy did

not reveal specific causes of death in late generation mTR null mice (data not shown).

### Decreased Body Weight

Body weight in mice typically increases in early and late postnatal development up to 1 year of age. Older animals show a terminal decline in body weight, and there is a positive correlation between body weight and life span (Goodrick, 1977; Ingram and Reynolds, 1987). Body weights were recorded at weekly intervals in aging mTR<sup>+/+</sup>, G1, and G6 mice throughout postnatal development. During the first 6 months, body weight curves were superimposable for all groups (Figure 4A). At both 10–14 and 15–18 months of age, the average body weight of the G6 animals was 20%–25% less than early generation mTR<sup>-/-</sup> and mTR<sup>+/+</sup> animals (Figure 4A,  $p < 0.0001$ ). Consistent with the decrease in body weight, a diminished fat cell layer between the dermis and the skeletal muscles was seen in the skin sections of old G6 animals (Figure 1F, asterisk), a finding considered to be a typical feature of aged human skin (Zivicnjak et al., 1997). In the gastrointestinal tract, villous atrophy and zonal blunting in the proximal intestine were detected in a subset (3/5) of the aged G6 animals by whole-mount staining and histological sections (Figures 4B–4E, representative samples shown). This disruption of the

Table 1. Summary of Phenotypic Analysis in Aging Mice

	mTR <sup>+/+</sup>	G3 mTR <sup>-/-</sup>	G6 mTR <sup>-/-</sup>
Body weight	Normal	Normal	20%–25% decreased in >6-month-old mice
Diabetes	Normal GTT	Normal GTT	Normal GTT
Osteoporosis	Normal X-ray	Normal X-ray	Normal X-ray
Artherosclerosis	None	None	None
Peripheral RBC & WBC counts	Normal	Normal	Normal
Blood chemistry	Normal profile	Normal profile	Normal profile
Cataract	15%	20%	10%
Male fecundity	12–15 months	6.5 months	Normally infertile, rarely successful in generating offspring
Hair graying and alopecia	25%	54%	60%
Skin histology	Normal	Decrease of hair follicles in anagen, increase in telogen	Decrease of hair follicles in anagen, increase in telogen, loss of subcutaneous fat
Ulcerative skin lesions	10%	31%	37%
Wound healing	Normal	Delayed reepithelialization	Delayed reepithelialization
Cancer incidence	3.3%	13%	19%
Life span (50% mortality mark)	24 months	24 months	18 months

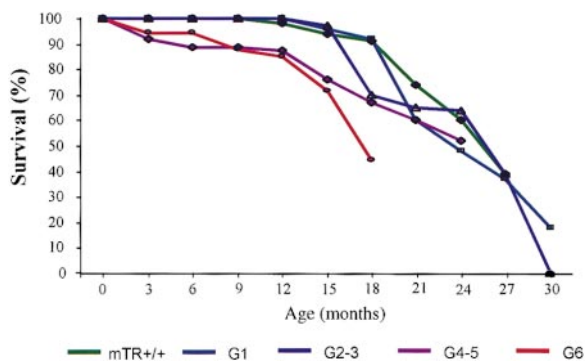


Figure 3. Loss of Telomere Ends Correlates with a Shortened Life Span

Survival curves of  $mTR^{+/+}$ , G1, G2-3, G4-5, and G6 mice, with percent of surviving animals plotted at 3-month intervals.

normal villous architecture is likely to contribute directly to body weight loss due to decreased nutritional absorption, an observation that has been described for aging rodents (Keelan et al., 1985; Chen et al., 1990).

#### Impaired Stress Response in Aged $mTR^{-/-}$ Mice

The limitation of cell replication by telomere shortening could affect the ability of the aging organism to respond to pathological conditions that provoke elevated cell turnover, as for example wounding, chronic hemolysis/bleeding, or infection. To address this possibility more directly, wound healing studies and the recovery potential of the hematopoietic system following blood cell ablation with 5-fluorouracil (5-FU) were monitored in young (1-3 months) and old (15-20 months)  $mTR^{+/+}$ , G3, and G6 mice.

#### Wound Healing

Four 3 mm punch biopsies were performed on the skin of the scapulae of mice housed in isolation, and the rate of wound healing was monitored by gross inspection and by serial histological examination. One day after wounding (PWD 1), the wounds of 15- to 18-month-old G3 and G6 mice exhibited delayed coagulum formation and remained opened and wet, while age-matched G1 and  $mTR^{+/+}$  mice achieved complete coagulum formation over all wounds (data not shown). The delay in wound closure was most apparent when wounds of PWD 4 and PWD 6 were compared, where day 6 wounds in the old G3 and G6 animals appeared macroscopically equivalent in size to day 4 wounds in age-matched G1 and  $mTR^{+/+}$  (Figures 5A and 5B, compare  $mTR^{+/+}$  day 4 to G6 day 6; G1 and G3 not shown). Histological sections through the healing wounds revealed a marked delay in wound reepithelialization in the old G3 and G6 mice (Figures 5C and 5D, G3 wounds not shown). Reepithelialization of wounds takes place by migration of keratinocytes from the wound edge toward the center and is known to be impaired in aged mice and humans (Holt et al., 1992; Ashcroft et al., 1997a, 1997b). In the older group of mice 2/16 (13%), wounds in  $mTR^{+/+}$  mice displayed incomplete reepithelialization at PWD 4, compared to 4/12 (33%) in G1, 7/10 (70%) in G3, and 12/16 (75%) in G6 mice ( $p = 0.001$ ). On PWD 4, epithelial gap diameters averaged 2097 and 2378  $\mu\text{m}$  in old G3 and G6

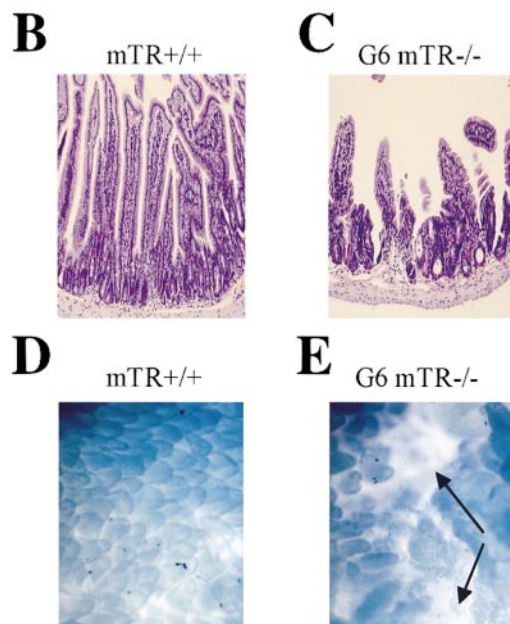
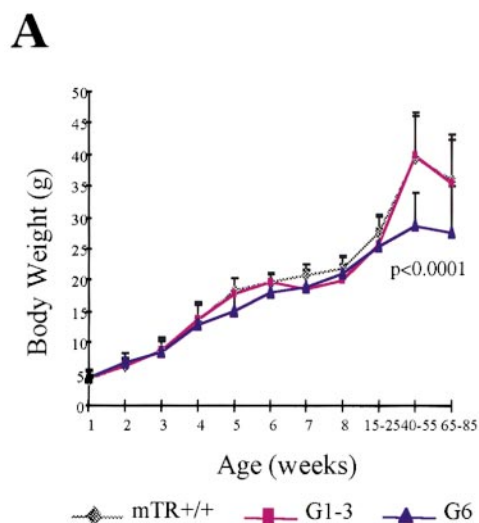


Figure 4. Reduced Body Weight and Villi Atrophy of the Small Intestine in Aged G6  $mTR^{-/-}$  Mice

(A) Body weights in  $mTR^{+/+}$  and  $mTR^{-/-}$  mice plotted as a function of age. Old G6 animals showed 20%–25% decrease in body weights. (B and C) H&E-stained cross sections of  $mTR^{+/+}$  and G6 duodenum at 18 months of age, showing blunted, markedly atrophic villi (20 $\times$  objective).

(D and E) Whole-mount preparations of  $mTR^{+/+}$  and G6 duodenum stained with methylene blue. Prominent areas of disorganized villi are present in the G6 duodenum (arrows).

animals, respectively. The two epithelial gaps present in old  $mTR^{+/+}$  animals possessed a mean gap diameter of 240  $\mu\text{m}$ . On average, the 15- to 18-month-old G3 and G6 mice required an additional 2 days to achieve full reepithelialization (6 versus 4 days for controls). It is interesting to note that, despite comparably short telomeres in old G3 and young G6 mice, impaired wound healing is observed only in aged  $mTR^{-/-}$  possessing critically shorter telomeres and accompanying telomere

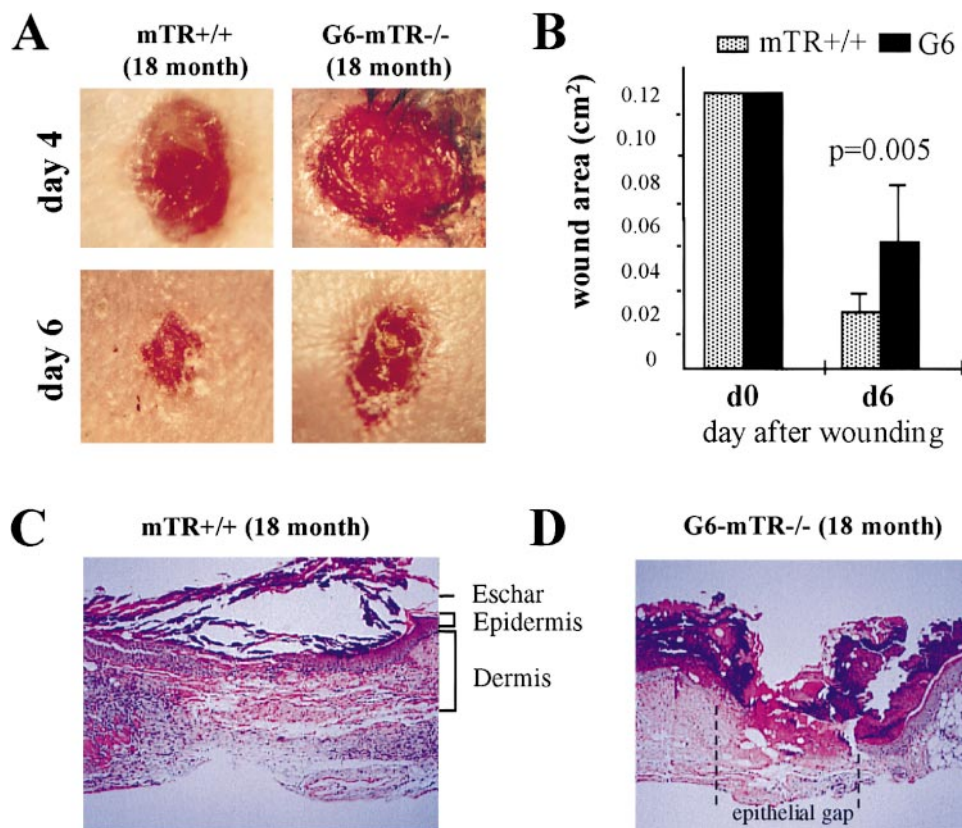


Figure 5. Delayed Wound Healing in Aged mTR<sup>-/-</sup> Mice

(A) Gross appearance of healing wounds of mTR<sup>+/+</sup> and G6 mice 4 and 6 days after wounding (2× objective).

(B) Wound areas at day 0 and 6 post wounding.

(C and D) Midtransverse sections (5 μm) through healing skin wounds at day 4 post wounding (H&E). Near complete reepithelization was detected in mTR<sup>+/+</sup> controls, in contrast to the prominent epithelial gap seen in G6 wounds (40× objective).

dysfunction (e.g., chromosomal fusions). Although the mechanistic basis for impaired wound healing is not well understood and thought to involve an interplay of cellular proliferation, growth factor production, and immune system dysfunction, the absence of significant differences in BrdU incorporation (data not shown) indicates that the impact of telomere shortening in wound repair of the aged mTR<sup>-/-</sup> mice is complex and extends beyond simple proliferation defects.

#### Response to Blood Cell Depletion

To further examine the capacity to cope with acute stress, peripheral blood cell kinetics and survival following 5-FU-induced ablation of the hematopoietic system were monitored in young and old mTR<sup>+/+</sup> and mTR<sup>-/-</sup> mice. mTR<sup>+/+</sup> mice will typically recover from a low dose of 5-FU (100 mg/kg body weight i.p.), and the ability to regain peripheral blood counts and body weight after 5-FU injection is a measure of the ability of the mice to respond to the induced stress. 5-FU exposure had no significant effect on body weight, WBC, hemoglobin, and the overall clinical status of young animals in all mTR<sup>-/-</sup> generations (Figures 6A–6C). In contrast, older mice (16–22 months) showed a decline in all peripheral blood cells with the lowest point occurring 6 days after injection (Figure 6B, WBC; Figure 6C, hemoglobin levels;

platelets not shown). Similarly, body weight curves showed a marked decline only in the old mice following 5-FU injection. Loss of body weight, which serves as an indicator of gastrointestinal defects and overall fitness, was more pronounced in old G6 compared to old mTR<sup>+/+</sup>, while G3 animals exhibited an intermediate phenotype (average loss of body weight 15% and 10%, respectively). The clinical appearance of the old G3 and G6 animals was markedly compromised, and subcutaneous injections of saline to maintain hydration of the animals had no therapeutic benefit. As a consequence of this generalized morbidity, three out of four old G6 and two out of five old G3 animals died on days 6–11. Notably, the mice that succumbed were those that showed the most profound decrease in WBC counts (specifically neutropenia) and body weight. In contrast, all of the old mTR<sup>+/+</sup> animals regenerated WBC counts by day 11, regained pretreatment body weights, and survived the treatment protocol. Red blood cells decreased in all treated animals (in part due to repeated phlebotomy for the peripheral blood count determinations); nevertheless, a delay in renewal was observed in old G3 and G6 but not in the mTR<sup>+/+</sup> or younger cohorts. Whereas three out of four old mTR<sup>+/+</sup> animals had regained sufficient hemoglobin levels (>10 g/dl) by day 11 after treatment, four out of five G3 and G6 animals

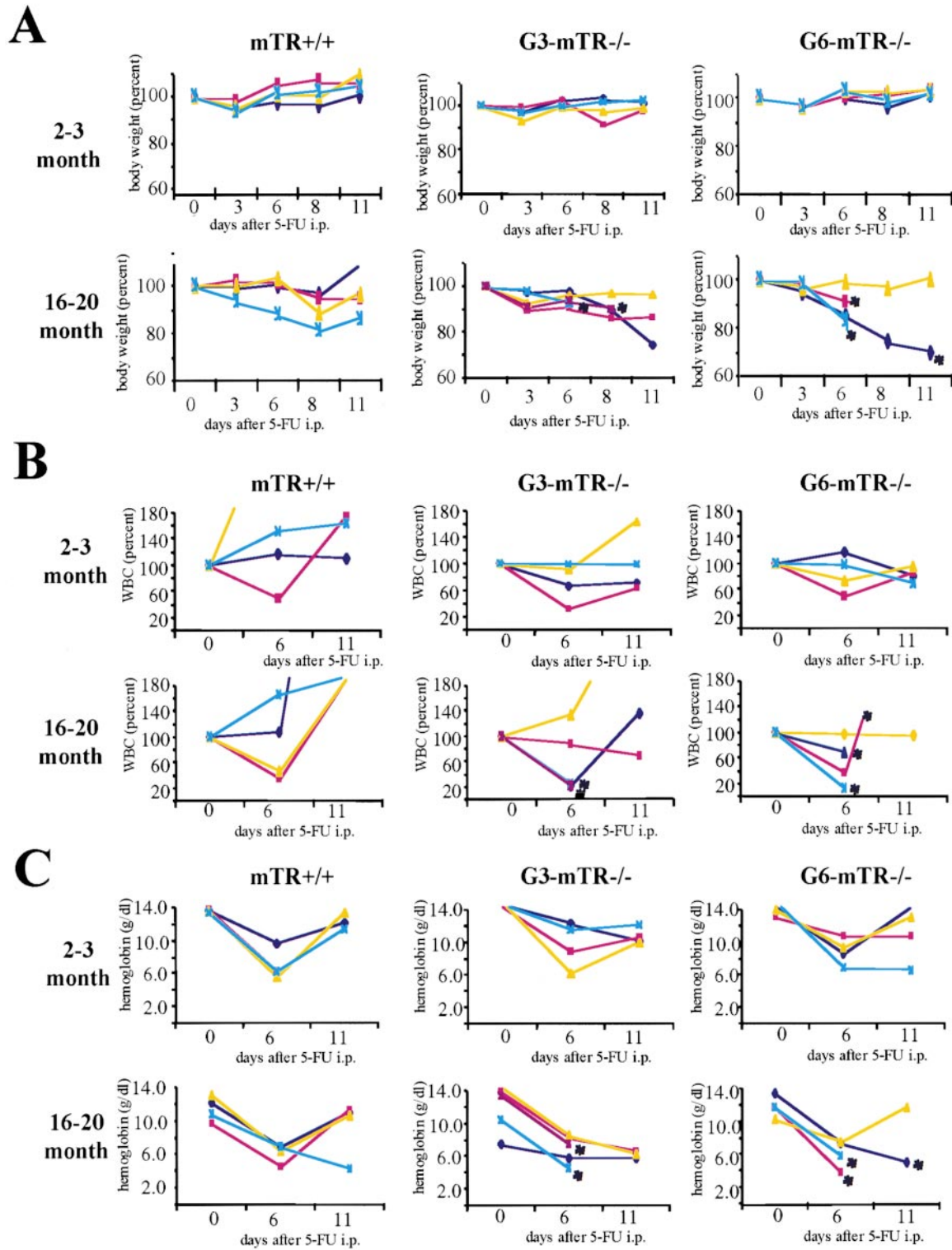


Figure 6. Age and Telomere Shortening Cooperate to Diminish Hematopoietic Reserve

Stress response to 5-FU treatment in young (2–3 months) and old (16–24 months) mTR<sup>+/+</sup>, G3, and G6 mice.

(A) Body weight, (B) peripheral WBC, and (C) hemoglobin levels (g/dl) plotted against days after 5-FU treatment; all parameters showed a dramatic reduction 6 days after treatment in old but not in young animals, with eventual recovery in mTR<sup>+/+</sup> animals. Asterisks indicate animal death: 0/4 in mTR<sup>+/+</sup>, 2/5 in G3, and 3/4 in G6 mice.

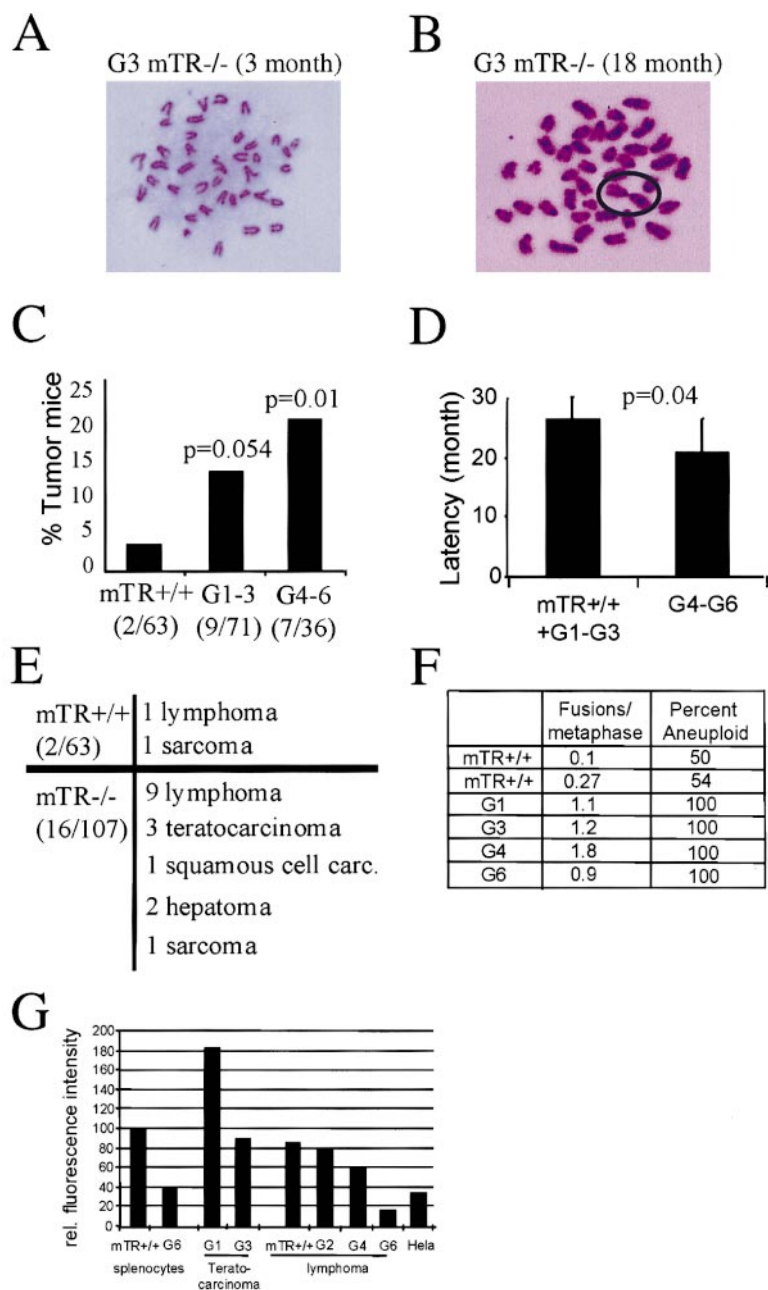


Figure 7. Genomic Instability and an Increased Incidence of Spontaneous Cancer in Aging mTR<sup>-/-</sup> Mice

(A and B) Representative metaphase spreads of lymphocytes. Circled area in (B) denotes chromosomal p-arm fusion in old G3 mouse.

(C) Incidence of macroscopically visible and clinically apparent spontaneous cancers.

(D) Age of onset of spontaneous cancers.

(E) Histological classification of spontaneous tumors.

(F) Cytogenetic analysis of representative spontaneously arising tumors.

(G) Telomere length in splenocytes of 18-month-old WT and G6 mice, and in teratocarcinomas and lymphomas derived from WT and mTR<sup>-/-</sup> mice. A human telomerase positive cervical carcinoma cell line (HeLa) is included for comparison of telomere lengths.

still showed critically low hemoglobin levels (<7 g/dl) (Figure 6C). Together these results demonstrate a diminished capacity of the aged telomerase-deficient mice to respond to a stress known to challenge the regenerative potential of the hematopoietic and gastrointestinal systems.

#### Increased Cytogenetic Abnormalities in Aged Late Generation mTR<sup>-/-</sup> Mice

Loss of telomere function in the mTR null mouse is associated with an increase in the frequency of chromosomal fusions and aneuploidy (Blasco et al., 1997; Lee et al., 1998). Since the studies described above demonstrated telomere loss as a function of age, it was possible that an increase in genomic instability with age could

contribute to the increase in phenotypic abnormalities. To examine this possibility, metaphase spreads were prepared from mitogen-stimulated peripheral white blood cells and splenic lymphocytes of young and old mTR<sup>+/+</sup> and G3 mice. No chromosomal fusions were observed in >30 metaphases derived from 2- to 3-month-old mTR<sup>+/+</sup> (data not shown) and G3 mice (Figure 7A). In >15-month-old G3 animals, an increased frequency of chromosomal fusions occurred (Figure 7B). While fusions in mTR<sup>+/+</sup> animals were rare and seen only in animals older than 24 months of age (frequency: 0.14 fusions per metaphase), chromosomal fusions were seen at a frequency of 0.45 fusions per metaphase in G3 mice older than 15 months. The increased incidence in chromosomal fusions with increasing age in the

mTR<sup>-/-</sup> mice is consistent with the observation that mTR<sup>-/-</sup> cell lines exhibit 50-fold more chromosomal fusions than mTR<sup>+/+</sup> cell lines under similar passage conditions (Hande et al., 1999).

#### Progressive Increase in the Rate of Spontaneous Tumor Formation in Successive Generations of mTR<sup>-/-</sup> Mice

Telomere loss and resultant chromosomal fusions can be consequences of cell growth and selection during tumorigenesis but may also play a role in increased cancer incidence in aging populations as speculated previously (Hastie et al., 1990; de Lange, 1995). The increase in chromosomal fusions in successive generations of young mTR null mice (G4 onward) and the age-dependent increase in chromosomal fusions in peripheral blood leukocytes of non-tumor-bearing aged G3 mice provided an opportunity to assess the role of loss of telomere function in cancer incidence. We monitored an aging population of mTR<sup>+/+</sup> and successive generations of mTR<sup>-/-</sup> mice for visible tumors. The tumors from both mTR<sup>+/+</sup> and mTR<sup>-/-</sup> mice were confirmed malignant by histological analysis. There was a 4- to 6-fold increase in the incidence of spontaneous cancers in mTR<sup>-/-</sup> animals (Figure 7C,  $p = 0.01$ , compare mTR<sup>+/+</sup> to G4–G6). Although the absolute number of tumors was low, it is noteworthy that the average age at tumor formation was younger in G4–G6 mice compared to mTR<sup>+/+</sup> and G1–G3 mice (20.5 versus 26.3 months, respectively,  $p = 0.04$ ; Figure 7D). In addition, the cancer rate in later generations (G4–G6) is higher than in G1–G3, even though many G6 mice have yet to reach an equivalently old age, during which the highest cancer rates were observed for mTR<sup>+/+</sup> and G1–G3 animals. (Thus, the cancer incidence reported here is likely to be an underestimate for the G4–G6 cohort.) The majority of tumor types originate from highly proliferative cell types (i.e., teratocarcinomas [germ cells], lymphomas [leukocytes], and squamous cell carcinomas [keratinocytes]). These cell types are likely to sustain the highest degree of telomere shortening with increasing age (Figure 7E). Together, these findings are consistent with the hypothesis that loss of telomere function and the resulting genetic instability that ensues facilitate the development of certain cancers. In line with this hypothesis, cytogenetic analysis of the tumors showed a 3- to 18-fold increase in the number of chromosomal fusions per metaphase and a 2-fold increase in the incidence of aneuploidy in mTR<sup>-/-</sup> tumors compared to mTR<sup>+/+</sup> tumors (Figure 7F). Although only two mTR<sup>+/+</sup> tumors were examined in this study, the low incidence of chromosomal fusions detected in these tumors was also observed in mTR<sup>+/+</sup> tumors derived from the *Ink4a*<sup>-/-</sup> mice (Greenberg and R. A. D., unpublished data). Flow-FISH analysis revealed shorter telomere ends in late generation mTR<sup>-/-</sup> tumors compared to mTR<sup>+/+</sup> tumors and early generation mTR<sup>-/-</sup> tumors (Figure 7G), indicating that loss of telomere function might contribute to tumorigenesis in these animals.

#### Discussion

Telomere and chromosome stability is necessary for cell viability. Previous studies showed that the mTR<sup>-/-</sup> mice

exhibit progressive telomere shortening and loss of proliferative cell types with each progressive generation (Blasco et al., 1997; Lee et al., 1998). Here we find that the ability of the mTR<sup>-/-</sup> mice to respond to various physiological stresses is compromised and declines with increasing age of the mouse. The mTR<sup>-/-</sup> mouse may be a good model for the age-associated decline in certain organ systems, particularly with regard to a hallmark feature of aging—a reduced capacity to tolerate acute stress. In addition, the increased tumor formation in the aging mTR<sup>-/-</sup> colony suggests that loss of telomere function may initiate genetic instability.

#### Telomere Length, Cellular Senescence, and Life Span

The correlation of telomere length and cellular senescence in human cells suggested that telomeres may somehow signal entry into cellular senescence in tissue culture (Harley et al., 1990; Allsopp et al., 1992). Recent experiments have provided significant support for this model (Bodnar et al., 1998; Vaziri and Benchimol, 1998; reviewed in Greider, 1998). The role of both cellular senescence and telomere length in aging is less clear. Many of the phenotypic consequences of *in vitro* cellular senescence are seen in aging tissue *in vivo* (Stanulis-Praeger, 1987; Campisi, 1997). However, given that life span determination likely has multiple inputs, it is not yet clear what role cellular senescence plays in determining organismal life span. While telomere length correlates well with cellular senescence, there is no evidence for a clear correlation at the organismal level with human life span. Further, mouse telomeres are significantly longer than human telomeres, and species differences in telomere length in the mouse do not correlate with life span (Greider, 1996). Thus, to the extent that there is a similar mechanism of life span determination between these two species, it is unlikely that telomere length is the driving determinant. Although some aspects of the mTR<sup>-/-</sup> mouse mimic age-associated disease, many signs and symptoms classically associated with premature aging mouse models were not evident in mTR<sup>-/-</sup> mice. In particular, there was no evidence of increased cataract formation, osteoporosis, glucose intolerance, or vascular disease. However, the decreased stress response seen in the mTR<sup>-/-</sup> mouse provides a good model to study the role of the age-related decline in stress response seen in humans.

#### Impaired Telomere Function and Stress Response

The aged, late generation mTR<sup>-/-</sup> mice showed diminished response to stress in several different settings. This decreased stress response could be a direct result of the decline in proliferative capacity of specific cell types or could indicate a more global organismal response to telomere shortening. Although studies from yeast show that telomere shortening only manifests itself after many cell divisions, the work presented here suggests that under some circumstances in mice, phenotypes can be observed that are not directly related to cell division. The inability of B and T cells from mTR<sup>-/-</sup> animals to respond to mitogenic stimulation is apparent in the first cell cycle after a mitogen is provided (Lee et

al., 1998). Since this phenotype can already be seen in G3 animals, and yet G4–G6 animals have viable B and T cells, the lack of response to mitogens cannot simply be due to reaching a critically short telomere length or a limit to cell division capacity. In a similar fashion, although the decreased response to stress described in this paper might be due in part to a diminished cell renewal capacity, it is also possible that short telomeres may directly impact upon more differentiated functions in certain tissues (e.g., cytokine production, signaling, etc.).

As individuals age, although baseline organ function remains adequate to sustain a healthy state, aged organs exhibit a markedly diminished capacity to cope with diverse acute and chronic stresses (Jazwinski, 1996). Impaired lymphocyte responsiveness in acute infections or diminished epithelial repair leading to chronic skin ulcers is often seen in aging individuals (Jurivich et al., 1997). Similarly, increased mortality and morbidity are evident following physiological stresses associated with chemotherapy or general surgery (Haeney, 1994). Although the mechanisms for how short telomeres block cell division and trigger apoptosis without ongoing cell division are not yet known, the  $mTR^{-/-}$  mouse provides an excellent model to study the possible role of telomere length in these cellular stress responses at the organismal level. This mouse model may thus shed light on this very important aspect of aging. Specifically, since the stress responses observed in old  $mTR^{+/+}$  and G1 mice were similar to those seen in young G6 mice, the aged late generation  $mTR^{-/-}$  mouse may provide an *in vivo* system to model age-related decline of gastrointestinal, hematopoietic, and cutaneous systems of humans.

#### Genetic Instability and Increased Cancer Incidence in Aging $mTR^{-/-}$ Animals

One of the functions of the telomere is to protect chromosomal ends from fusions and other rearrangements. Previous studies employing human fibroblasts have established a correlation between a progressive decline in telomere length during passage and an increased incidence of telomere fusions (Counter et al., 1992; Vaziri et al., 1993). Similarly, a reduction in telomere length in successive generations of  $mTR$  null mice is associated with Robertsonian end-to-end fusions (Blasco et al., 1997; Lee et al., 1998). The fact that telomeres are shortened in a variety of human cancers in which chromosomal abnormalities are also commonly present has fueled speculation that telomere erosion might be a risk factor for the genesis of some tumors (Pathak et al., 1994; de Lange, 1995).

We found a correlation between an age- and generation-dependent increase in cytogenetic abnormalities (consistent with telomere dysfunction, e.g., end-to-end fusions) and an increase in the incidence of spontaneous cancers. This link is supported by the earlier age of onset of tumors in the later generations and by the spectrum of cancer types and their emergence from telomere-dependent organs (lymphoid, testes, and skin; testis not shown). Particularly striking is the high incidence of teratocarcinomas in the  $mTR^{-/-}$  mice in light of the extremely low incidence of such tumors in our large  $mTR^{+/+}$  mouse colony over many years. Such a correlation is consistent with the hypothesis that telomere erosion may initiate genetic instability that leads to cancer.

At face value, the increased tumor incidence seems to contradict the decrease in tumor formation expected from the loss of cell viability associated with telomere dysfunction. It also appears confusing in light of the frequent upregulation of telomerase postcrisis (Harley and Sherwood, 1997; Shay, 1997) or the ability of telomerase to facilitate transit through crisis (Counter et al., 1992; de Lange, 1994; Weinberg, 1998). Moreover, we have documented a significant decrease in tumor incidence in mice doubly null for  $mTR^{-/-}$  (G4 onward) and the *INK4a* tumor suppressor gene (Greenberg and R. A. D., unpublished data). The difference in these studies may be that in early divisions loss of telomere function can initiate genetic instability, while at later points in tumor progression the absence of telomerase inhibits long-term growth. Thus, while telomerase inhibition may be a valid approach in the treatment of established tumors, age-dependent telomere shortening may be an important risk factor for cancer in settings of bypass of the mortality I checkpoint. Together, these studies underscore the complex relationship between telomeres, tumorigenesis, and aging and highlight the need to conduct relevant studies in intact organisms against the backdrop of defined cancer-relevant mutations.

#### Experimental Procedures

##### $mTR$ Null Mouse and Mating Scheme

Production of the  $mTR$  null mouse has been described previously (Blasco et al., 1997). Generation 1 (G1) knockout animals and  $mTR^{+/+}$  control animals were derived from heterozygous intercrosses (mixed genetic background). Mating of G1- $mTR^{-/-}$  animals to each other generated G2 animals. Following this mating scheme,  $mTR^{-/-}$  animals up to the sixth generation (G6) were produced. All animals were kept in the same room and fed *ad libitum*. Routine serologies confirmed that all mice remained pathogen free over the entire study period.

##### Alopecia and Hair Graying

Hair graying was quantitated at different parts of the animal's body by estimating the percentage of gray hairs, and the results were classified as either mild (<10%), medium (10%–30%), or severe (>30%) hair graying. Alopecia was quantitated by counting hairs in one square centimeter areas of the animal's back (Courtois et al., 1995). Quantification of hair follicles in the telogen or anagen phase of hair growth was performed on hematoxylin and eosin (H&E) stained cross sections of the animal's dorsal skin.

##### Skin Analysis and Wound Healing Studies

Four 3 mm full thickness punch biopsies extending through the epidermis and dermis to the panniculus carnosus were made overlying the scapulas using circular skin biotomies. Wounds were created in four different animals per group (2- to 3-month and 15- to 18-month-old  $mTR^{+/+}$ , G1, G3, and G6) after chemical depilation. Wound sizes were measured with a 2 $\times$  objective. At 4 and 6 days after wounding, 5  $\mu$ m midtransverse paraffin sections were stained with H&E. Epithelial gap diameters were determined by optical micrometer measurements using calibrated 10 $\times$  and 20 $\times$  objectives at post wounding day 4.

##### 5-Fluorouracil Study

Two-month and 16- to 20-month-old  $mTR^{+/+}$ , G3, and G6 animals were treated with an *i.p.* bolus injection of 5-fluorouracil (5-FU) at a dose of 100 mg/kg body weight. Peripheral blood was obtained via tail bleeds before injection and on days 6 and 11 after injection. Bleeding was terminated upon withdrawal of 150  $\mu$ l blood volume. Peripheral blood counts and white blood cell differentials were analyzed by an automated CBC analyzer and by microscopic examination.

#### Gastrointestinal Tract and Overall Organ Assessments

Whole-mount staining of the intestine was performed on 1 cm<sup>2</sup> preparations as described previously (Pretlow et al., 1991). For histology, the organs were fixed in 10% formalin, and 5  $\mu$ m paraffin sections were stained with H&E. Serum analysis for LDH, bilirubin, AST, ALT, total protein, albumin, alkaline phosphatase, GGT, and cholesterol, uric acid, creatinine, calcium, and serum electrolytes was analyzed using a DAX analyzer. Glucose tolerance tests (2 mg glucose/g body, i.p.) were performed after a 16 hr fast on mTR<sup>+/+</sup>, G3, and G6 animals. Bone density radiographs were taken on dissected mouse femurs of 2- to 3-month-old and 18- to 24-month-old mTR<sup>+/+</sup>, G3, and G6 animals (three different animals per group) using AD Mammo Fine film (Fuji).

#### Telomere Length Analysis

Telomere length analysis was performed on peripheral white blood cells by flow-cytometry-FISH as recently described (Hultdin et al., 1998; Rufer et al., 1998). Peripheral blood cells were obtained after tail bleeds (500  $\mu$ l) and red cell lysis with ammonium chloride. Day to day variations in the linearity of the flow cytometer were controlled by the use of FITC-labeled fluorescence beads (Flow Cytometry Standards Corporation, San Juan, Puerto Rico).

#### Metaphase Spreads

Splenocytes and peripheral blood cells were stimulated with mitogens (5  $\mu$ g ConA/ml + LPS [100  $\mu$ g/ml]) for 24 hr followed by incubation in 0.1 g/ml colcemid for 60 min. Tumor cells were treated for 1–4 hr with colcemid, depending on the growth characteristics. After spinning at 1000 rpm, the cells were incubated in 75 mmol KCl for 15 min, spun again, and fixed in methanol:glacial acetic acid (3:1, v:v). Metaphases were dropped from 1 m onto frosted microscope slides positioned at a 45° angle. Giemsa staining was performed according to standard protocols. Quantification of fusions and photographs were taken with 60 $\times$  and 100 $\times$  objectives.

#### Cancer Incidence

Aging mice were inspected weekly for macroscopically visible tumors or palpable abdominal tumors. Tumor-bearing mice were anesthetized, and tumor biopsies were taken for histology and metaphase preparations. All cancer diagnoses were confirmed histologically. Animals that were found dead were dissected and inspected for macroscopically visible tumors.

#### Statistics

Unpaired t test and Fisher's exact test were used for calculation of p values.

#### Acknowledgments

We thank Steven Artandi, Lynda Chin, Ronan O'Hagan, and Nicole Schreiber-Agus for critical reading of the manuscript, and B. Furman, K. E. Cedeno-Baier, L. Husted, and S. Rao for excellent technical assistance. The work was supported by grants from the National Institutes of Health and American Heart Association grant-in-aid to R. A. D.; R. A. D. is an American Cancer Society Research Professor. Support from the Dana Farber Cancer Institute Cancer Core grant to R. A. D. is acknowledged. K. L. R. is supported by the Deutsche Forschungsgemeinschaft (Ru 745/1-1), and C. G. is supported by the National Institutes of Health. M. B. is supported by the Ministry of Education and Culture of Spain and by the Department of Immunology and Oncology (CSIC-Pharmacia and Upjohn).

Received December 29, 1998; revised January 28, 1999.

#### References

Allsopp, R.C., Vaziri, H., Patterson, C., Goldstein, S., Younglai, E.V., Fletcher, A.B., Greider, C.W., and Harley, C.B. (1992). Telomere length predicts replicative capacity of human fibroblasts. *Proc. Natl. Acad. Sci. USA* **89**, 10114–10118.

Ashcroft, G.S., Horan, M.A., and Ferguson, M.W. (1997a). The effects of ageing on wound healing: immunolocalization of growth factors

and their receptors in a murine incisional model. *J. Anat.* **190**, 351–365.

Ashcroft, G.S., Horan, M.A., and Ferguson, M.W. (1997b). Aging is associated with reduced deposition of specific extracellular matrix components, an upregulation of angiogenesis, and an altered inflammatory response in a murine incisional wound healing model. *J. Invest. Dermatol.* **108**, 430–437.

Austriaco, N.R., and Guarente, L.P. (1997). Changes of telomere length cause reciprocal changes in the life span of mother cells in *Saccharomyces cerevisiae*. *Proc. Natl. Acad. Sci. USA* **94**, 9768–9772.

Blasco, M.A., Lee, H.W., Hande, M.P., Samper, E., Lansdorf, P.M., DePinho, R.A., and Greider, C.W. (1997). Telomere shortening and tumor formation by mouse cells lacking telomerase RNA. *Cell* **91**, 25–34.

Bodnar, A.G., Ouellette, M., Frolkis, M., Holt, S.E., Chiu, C.P., Morin, G.B., Harley, C.B., Shay, J.W., Lichtsteiner, S., and Wright, W.E. (1998). Extension of life-span by introduction of telomerase into normal human cells. *Science* **279**, 349–352.

Campisi, J. (1997). The biology of replicative senescence. *Eur. J. Cancer* **33**, 703–709.

Campisi, J. (1998). The role of cellular senescence in skin aging. *J. Invest. Dermatol. Symp. Proc.* **3**, 1–5.

Chang, E., and Harley, C.B. (1995). Telomere length and replicative aging in human vascular tissues. *Proc. Natl. Acad. Sci. USA* **92**, 11190–11194.

Chen, T.S., Currier, G.J., and Wabner, C.L. (1990). Intestinal transport during the life span of the mouse. *J. Gerontol.* **45**, 129–133.

Cooke, H.J., and Smith, B.A. (1986). Variability at the telomeres of the human X/Y pseudoautosomal region. *Cold Spring Harb. Symp. Quant. Biol.* **51 Pt 1**, 213–219.

Counter, C.M. (1996). The roles of telomeres and telomerase in cell life span. *Mutat. Res.* **366**, 45–63.

Counter, C.M., Avilion, A.A., LeFeuvre, C.E., Stewart, N.G., Greider, C.W., Harley, C.B., and Bacchetti, S. (1992). Telomere shortening associated with chromosome instability is arrested in immortal cells which express telomerase activity. *EMBO* **11**, 1921–1929.

Courtois, M., Loussouarn, G., Hourseau, C., and Grollier, J.F. (1994). Hair cycle and alopecia. *Skin Pharmacol.* **7**, 84–89.

Courtois, M., Loussouarn, G., Hourseau, C., and Grollier, J.F. (1995). Ageing and hair cycles. *Br. J. Dermatol.* **132**, 86–93.

de Lange, T. (1994). Activation of telomerase in a human tumor. *Proc. Natl. Acad. Sci. USA* **91**, 2882–2885.

de Lange, T. (1995). Telomere dynamics and genomic instability in human cancer. In *Telomeres*, E.H. Blackburn and C.W. Greider, eds. (Cold Spring Harbor, NY: Cold Spring Harbor Laboratory Press), pp. 265–293.

de Lange, T. (1998). Telomeres and senescence: ending the debate. *Science* **279**, 334–335.

D'Mello, N.P., and Jazwinski, S.M. (1991). Telomere length constancy during aging of *Saccharomyces cerevisiae*. *J. Bacteriol.* **173**, 6709–6713.

Dorman, J.B., Albinder, B., Shroyer, T., and Kenyon, C. (1995). The *age-1* and *daf-2* genes function in a common pathway to control the life span of *Caenorhabditis elegans*. *Genetics* **141**, 1399–1406.

Effros, R.B., Allsopp, R., Chiu, C.P., Hausner, M.A., Hirji, K., Wang, L., Harley, C.B., Villeponteau, B., West, M.D., and Giorgi, J.V. (1996). Shortened telomeres in the expanded CD28<sup>-</sup>CD8<sup>+</sup> cell subset in HIV disease implicate replicative senescence in HIV pathogenesis. *AIDS* **10**, F17–22.

Frenck, R.W., Blackburn, E.H., and Shannon, K.M. (1998). The rate of telomere sequence loss in human leukocytes varies with age. *Proc. Natl. Acad. Sci. USA* **95**, 5607–5610.

Goodrick, C.L. (1977). Body weight change over the life span and longevity for C57BL/6J mice and mutations which differ in maximal body weight. *Gerontology* **23**, 405–413.

Greenberg, R.A., Allsopp, R.C., Chin, L., Morin, G.B., and DePinho, R.A. (1998). Expression of mouse telomerase reverse transcriptase during development, differentiation and proliferation. *Oncogene* **16**, 1723–1730.

## GENE THERAPY

# Telomerase gene therapy rescues telomere length, bone marrow aplasia, and survival in mice with aplastic anemia

Christian Bär,<sup>1</sup> Juan Manuel Povedano,<sup>1</sup> Rosa Serrano,<sup>1</sup> Carlos Benitez-Buelga,<sup>2</sup> Miriam Popkes,<sup>1</sup> Ivan Formentini,<sup>3</sup> Maria Bobadilla,<sup>4</sup> Fatima Bosch,<sup>5</sup> and Maria A. Blasco<sup>1</sup>

<sup>1</sup>Telomeres and Telomerase Group, Molecular Oncology Program and <sup>2</sup>Human Genetics Group, Spanish National Cancer Research Centre, Madrid, Spain; <sup>3</sup>Roche Pharma Research and Early Development, Neuroscience, Ophthalmology, and Rare Disease, Roche Innovation Center and <sup>4</sup>Roche Extending the Innovation Network Academia Partnering Program, F. Hoffmann-La Roche, Basel, Switzerland; and <sup>5</sup>Centre of Animal Biotechnology and Gene Therapy, Department of Biochemistry and Molecular Biology, School of Veterinary Medicine, Universitat Autònoma de Barcelona, Bellaterra, Spain

### Key Points

- Telomerase gene therapy in a mouse model of aplastic anemia targets the bone marrow and provides increased and stable telomerase expression.
- Telomerase expression leads to telomere elongation and subsequently to the reversal of aplastic anemia phenotypes.

**Aplastic anemia is a fatal bone marrow disorder characterized by peripheral pancytopenia and marrow hypoplasia. The disease can be hereditary or acquired and develops at any stage of life. A subgroup of the inherited form is caused by replicative impairment of hematopoietic stem and progenitor cells due to very short telomeres as a result of mutations in telomerase and other telomere components. Abnormal telomere shortening is also described in cases of acquired aplastic anemia, most likely secondary to increased turnover of bone marrow stem and progenitor cells. Here, we test the therapeutic efficacy of telomerase activation by using adeno-associated virus (AAV)9 gene therapy vectors carrying the telomerase *Tert* gene in 2 independent mouse models of aplastic anemia due to short telomeres (*Trf1*- and *Tert*-deficient mice). We find that a high dose of AAV9-*Tert* targets the bone marrow compartment, including hematopoietic stem cells. AAV9-*Tert* treatment after telomere attrition in bone marrow cells rescues aplastic anemia and mouse survival compared with mice treated with the empty vector. Improved survival is associated with a significant increase in telomere length in peripheral blood and bone marrow cells, as well as improved blood counts. These findings indicate that telomerase**

**gene therapy represents a novel therapeutic strategy to treat aplastic anemia provoked or associated with short telomeres. (*Blood*. 2016;127(14):1770-1779)**

## Introduction

Aplastic anemia is a potentially life-threatening, rare, and heterogeneous disorder of the blood in which the bone marrow cannot produce sufficient new blood cells due to a marked reduction of immature hematopoietic stem and progenitor cells (HSPCs).<sup>1,2</sup> The main disease manifestations are pancytopenia and marrow hypoplasia, which can emerge at any stage of life but are more frequent in young individuals (age 10-25 years) and in the elderly (>60 years).<sup>3</sup> Aplastic anemia can be acquired or inherited. The acquired type is often of idiopathic origin and involves autoimmune processes but can also be triggered by environmental factors such as exposure to radiation, toxins, and viral infections.<sup>4</sup> The congenital form is rarer, and mutations in more than 30 genes involved in DNA repair, ribosome biogenesis, and telomere maintenance pathways have been identified to date.<sup>5</sup> A frequently observed clinical feature of aplastic anemia is the presence of short telomeres in subpopulations of peripheral blood cells (neutrophils in particular; less prominent in lymphocytes),<sup>6</sup> even in the absence of mutations in the telomere maintenance machinery.

Telomeres, the termini of vertebrate chromosomes, are specialized nucleoprotein structures composed of tandem repeat sequences (TTAGGG in vertebrates) bound by a 6-protein complex (TRF1,

TRF2, TIN2, RAP1, TPP1, and POT1) known as shelterin.<sup>7,8</sup> Telomeres are essential for chromosome integrity by preventing telomere fusions and telomere fragility. Telomere length is controlled by the ribonucleoprotein enzyme telomerase, which can add telomeric sequences onto telomeres de novo. Because telomeres shorten with every cell division (a phenomenon known as the “end replication problem”) and somatic cells do not express sufficient telomerase to compensate for this, telomeres shorten throughout life. When telomeres reach a critically short length, their protective function is impaired, eliciting a persistent DNA-damage response at chromosome ends, which leads to cellular senescence or cell death.<sup>9,10</sup> Hematopoietic stem cells, in contrast to most somatic cells, can activate telomerase; however, this is insufficient to prevent telomere attrition with aging, thus eventually leading to loss of the regeneration potential of hematopoietic stem cells.<sup>11</sup> In line with this, recipients of bone marrow transplants have shorter telomeres than their donors, suggesting that telomerase cannot fully compensate for the increased cell proliferation that occurs during the engraftment phase of the transplanted bone marrow.<sup>12</sup> Telomeres also show an accelerated rate of shortening in patients with aplastic anemia compared with

Submitted August 31, 2015; accepted January 27, 2016. Prepublished online as *Blood* First Edition paper, February 22, 2016; DOI 10.1182/blood-2015-08-667485.

© 2016 by The American Society of Hematology

healthy individuals, most likely due to a higher than normal number of cell divisions in the aplastic anemia cases.<sup>13</sup>

Accelerated telomere shortening due to defects in telomerase or other telomere maintenance genes prematurely limits the proliferation potential of cells, including stem cells, leading to decreased tissue renewal capacity.<sup>9,14</sup> Highly proliferative tissues such as the hematopoietic system are particularly vulnerable to defects in telomere maintenance genes, leading to severe disorders such as aplastic anemia.<sup>15</sup> As an example, the telomeropathy dyskeratosis congenita (DKC) has been linked to mutations in 11 genes that encode components of the telomerase complex (*TERT*, *TERC*, *DKC1*, *NOP10*, and *NHP2*) or of the telomere capping complex shelterin (*TIN2*). Other genes altered in DKC encode for accessory proteins important for telomerase assembly and trafficking (*CTCI*, *ACD7* [alias *TPPI1*], and *TCABI*) or for telomere replication (*RTEL1*).<sup>16</sup> Mutated *PARN* was also recently linked to reduced messenger RNA (mRNA) levels of several key genes in telomere maintenance.<sup>17</sup> In all these cases, DKC is characterized by very short telomeres. DKC is a multisystem syndrome comprising diverse clinical features such as nail dystrophy, oral leukoplakia, abnormal skin pigmentation, and cerebellar hypoplasia.<sup>16</sup> The most severe complication, however, is the development of aplastic anemia in 80% of the cases, underlining that the clinical features are caused by excessive telomere shortening that eventually leads to the exhaustion of the stem cell reserve.<sup>5</sup>

These findings suggest that telomerase activation could be a good therapeutic strategy to treat those forms of aplastic anemia associated with a limited blood-forming capacity due to the presence of very short telomeres. We have previously developed a telomerase (*Tert*) gene therapy using adeno-associated virus (AAV)9 vectors,<sup>18</sup> which attenuated or reverted aging-associated telomere erosion in peripheral blood mononuclear cells (PBMCs).<sup>18</sup>

To test the efficacy of this strategy in the treatment of aplastic anemia, we first used a mouse model of aplastic anemia generated by us in which we depleted the TRF1 shelterin protein specifically in the bone marrow, leading to a bone marrow phenotype that recapitulates the main pathological findings of human aplastic anemia patients, including extreme telomere shortening.<sup>19,20</sup> In particular, partial depletion of the *Trf1* gene specifically in bone marrow causes severe telomere uncapping and provokes a persistent DNA-damage response at telomeres, which in turn leads to a fast clearance of those HSPCs deficient for *Trf1*. In this context, the remaining HSPCs that did not delete the *Trf1* gene undergo additional rounds of compensatory proliferation to regenerate the bone marrow, leading to very rapid telomere attrition. Thus, partial depletion of the bone marrow stem cell and progenitor compartments by *Trf1* deletion recapitulates the compensatory hyperproliferation and short telomere phenotype observed after bone marrow transplant or in other acquired forms of aplastic anemia, as well as in patients due to mutations in telomere maintenance genes. Interestingly, this mouse model allows adjustment of the rate of telomere shortening by modulating the frequency of *Trf1* deletion-mediated HSPC depletion, thus controlling the onset of bone marrow aplasia and pancytopenia.<sup>19,20</sup>

As an additional model to mimic the presence of very short telomeres specifically in the bone marrow, we transplanted irradiated wild-type mice with bone marrow from late (third)-generation (G3) telomerase-deficient *Tert*-knockout mice, which have short telomeres due to telomerase deficiency during 3 mouse generations.

Here, we tested telomerase activation by using gene therapy AAV vectors in both mouse models of aplastic anemia produced by short telomeres. Our results show that telomerase treatment is sufficient to attenuate telomere attrition and HSPC depletion with time, thus significantly preventing death by bone marrow failure.

## Material and methods

### Study approval

All experimental procedures with mice (*Mus musculus*) were approved by the Spanish National Cancer Research Center Instituto de Salud Carlos III Ethics Committee for Research and Animal Welfare. Mice were treated in accordance to the Spanish laws and the Federation of European Laboratory Animal Science Associations guidelines (approval file number CBA PA 87\_2012).

### Mice and animal procedures

Mice of pure C57/BL6 background were produced and housed at the specific-pathogen-free animal house of the Spanish National Cancer Research Center in Madrid, Spain. *Trf1*<sup>lox/lox</sup> *Mx1-Cre* and *Trf1*<sup>lox/lox</sup> *Mx1-wt* mice were generated as described previously.<sup>21</sup> First-generation (G1) *Tert*<sup>-/-</sup> mice were generated by intercrossing *Tert*<sup>+/-</sup>. G3 *Tert*<sup>-/-</sup> mice were obtained by intercrossing G1 mice (to give second-generation [G2] mice) and subsequently intercrossing G2 mice.<sup>22</sup> Ten-week-old *Trf1*<sup>lox/lox</sup> *Mx1-Cre* or G3 *Tert*<sup>-/-</sup> mice were used as bone marrow donors for transplant into 8-week-old lethally irradiated (12 Gy) wild-type mice as described previously.<sup>19,23</sup> Two million cells were transplanted via tail vein injection at a donor-to-recipient ratio of 1:8, and mice were left for 30 days to allow bone marrow reconstitution. To induce Cre expression, mice were intraperitoneally injected with 15  $\mu$ g/g body weight of polyinosinic: polycytidylic acid (pI:PC; Sigma-Aldrich) 3 times per week for a total of 5 weeks. After 1 week, mice were treated with the AAV9-*Tert* or AAV9-empty vector. Vectors were administered via tail vein injection at a concentration of  $3.5 \times 10^{12}$  viral genomes per mouse.

### Gene therapy vector production

Viral vectors were generated<sup>24</sup> and purified as described previously.<sup>25</sup> Briefly, vectors were produced through triple transfection of HEK293T. Expression cassettes were under the control of the cytomegalovirus promoter and contained an SV40 polyA signal for *EGFP* and the cytomegalovirus promoter, and a 3' untranslated region of the *Tert* gene as polyA signal for *Tert*. AAV9 particles were purified using 2 cesium chloride gradients, dialyzed against phosphate-buffered saline (PBS) and filtered.<sup>25</sup> Viral genome particle titers were determined by a quantitative real-time polymerase chain reaction (PCR) method.<sup>26</sup>

### Histology

Bone marrow samples (sternum or tibia bone) were fixed in 4% paraformaldehyde and paraffin embedded after decalcification. Tissue sections (5  $\mu$ m) were stained with hematoxylin and eosin. Immunohistochemistry was performed on deparaffinized sections. After antigen retrieval, samples were stained with anti-enhanced green fluorescent protein (EGFP) (rabbit anti-EGFP, 1:200, ab290; Abcam). EGFP-positive cells were counted in a semiautomated way using ImageJ software.

### FACS

For sorting of HSPCs, whole bone marrow cells were extracted from the long bones (femur and tibia) as described previously.<sup>23</sup> Erythrocytes were lysed for 10 minutes in 10 mL of erythrocyte lysis buffer (Roche), washed once with 10 mL of PBS, and resuspended in fluorescence-activated cell sorting (FACS) buffer (PBS, 2 mM EDTA, 0.3% bovine serum albumin) containing Fc-block (1:400) at a concentration of 5 to  $10 \times 10^6$  cells per 100  $\mu$ L. Cells were incubated for 10 minutes and washed once in FACS buffer. Cells were then resuspended in FACS buffer at 20 to  $25 \times 10^6$  cells per milliliter, and the antibody cocktail was added as follows: anti-Sca-1-PerCP-Cy5.5 (1:200), lin cocktail-eFluor450 (1:50) (all eBioscience), and anti-c-kit-APC-H7 (1:100) (BD Pharmingen). Cells were incubated for 30 minutes. After washing cells twice with PBS, 2 mL of 4,6 diamidino-2-phenylindole (DAPI; 2 mg/mL) was added and cells were sorted in a FACS Aria IIU (Becton Dickinson, San Jose, CA) into HSPCs (lin<sup>-</sup>, Sca-1<sup>+</sup>, and c-kit<sup>+</sup>) and lineage-positive fractions.

### Colony-forming assay

A short-term colony-forming assay was performed by plating  $1 \times 10^4$  and  $2 \times 10^4$  freshly isolated mononucleated bone marrow cells in 35 mm dishes containing MethoCult media (both STEMCELL Technologies) following the manufacturer's protocol. All experiments were performed in duplicate, and the number of colonies was counted after 12 days of incubation at 37°C.

### Blood counts

Peripheral blood was drawn from the facial vein (~50  $\mu$ L) and collected into anticoagulation tubes (EDTA). Blood counts were determined using an Abacus Junior Vet veterinary hematology analyzer.

### Quantitative real-time PCR and western blot analysis

Total RNA from whole bone marrow extracts or from bone marrow cells sorted by FACS was isolated using QIAGEN's RNeasy Mini Kit according to the manufacturer. Quantitative real-time PCR was performed using an ABI PRISM 7700 or QuantStudio 6 Flex (both Applied Biosystems). Primer sequences for *Tert* and reference genes *Act1* and *TBP* are as follows: *Tert*-forward 5'GGATTGCCACTGGCTCCG; *Tert*-reverse 5'TGCCTGACCTCTCTGTGAC; *actin*-forward 5'GGCACCACACCTTCTACAATG; *actin*-reverse 5'TGGTGGTGAAGCTGTAG; *TBP*-forward 5'CTTCCTGCCACAATGTCACAG; *TBP*-reverse 5'CCTTTCTCATGCTTCTCTCTG.

### Q-FISH telomere analysis

Quantitative FISH (Q-FISH) on paraffin-embedded tissue sections was performed as described previously.<sup>27</sup> Confocal images were acquired as stacks every 0.5  $\mu$ m for a total of 1.5  $\mu$ m using a Leica SP5-MP confocal microscope, and maximum projections were done with the Leica Application Suite-Advanced Fluorescence software. Telomere signal intensity was quantified in at least 6 images per mouse using Definiens software, with a specific script allowing for individual spot background correction.

High-throughput (HT)-Q-FISH on peripheral blood leukocytes was done using 120 to 150  $\mu$ L of blood as described previously.<sup>28</sup> Confocal images were captured using the Opera High-Content Screening system (Perkin Elmer). Telomere length values were analyzed using individual telomere spots (>10 000 telomere spots per sample). The average fluorescence intensities of each sample were converted into kilobases using L5178-R and L5178-S cells as calibration standards, which have stable telomere lengths of 79.7 kb and 10.2 kb, respectively.<sup>29</sup> Samples were analyzed in duplicate.

Real-time PCR-based measurement of relative telomere length was done on genomic DNA isolated from whole bone marrow samples following a previously described protocol.<sup>30,31</sup>

## Results

### AAV9-*Tert* targets bone marrow and hematopoietic stem cells

First, we tested the ability of AAV9 vectors to transduce bone marrow cells upon mouse IV injection. In particular, to determine the location and percentage of transduced cells, we first treated wild-type mice with an AAV9-EGFP reporter virus ( $3.5 \times 10^{12}$  viral genomes per mouse) via tail vein injections. We found that 2% of the BM cells were positive for EGFP upon immunohistochemistry with anti-EGFP antibodies in in middle bone sections, and this increased to 10% in bone regions adjacent to the joints, which showed the highest AAV9 transduction (Figure 1A-B). We then injected wild-type mice with the same amount of AAV9-*Tert* particles and determined *Tert* mRNA expression by quantitative real-time PCR in whole bone marrow isolates at 2 weeks and 8 months after virus injection. At 2 weeks posttreatment with the AAV9 vectors, *Tert* mRNA expression was significantly increased in the AAV9-*Tert*-treated mice compared with those treated with the AAV9-empty vector, and this increased expression was maintained up

to 8 months after the initial treatment (Figure 1C-E). In agreement with the known tropism of the AAV9 serotype, we found a stronger induction of *Tert* in organs such as heart and liver, which are preferential AAV9 targets (supplemental Figure 1, available on the Blood Web site).<sup>32</sup> We then studied *Tert* mRNA expression specifically in the blood-forming compartments of the bone marrow. To this end, we performed FACS of c-kit<sup>+</sup> and Sca-1<sup>+</sup> HSPCs and lin<sup>+</sup> lineage-committed cells. We found a significant increase in *Tert* mRNA in HSPCs (10-fold) and lineage-committed bone marrow cells (3.5-fold) in AAV9-*Tert*-treated mice compared with mice treated with the empty vector (Figure 1F-G), demonstrating that bone marrow cells, including HSPCs, are targeted by *Tert* gene therapy. Of note, the higher expression in whole bone marrow compared with isolated hematopoietic cells (HPSCs and lin<sup>+</sup> cells) could suggest that additional bone marrow cells corresponding to the stroma (ie, adipocytes) may also be infected. In this regard, we previously demonstrated that adipocytes are efficiently targeted by AAV9.<sup>33</sup> Moreover, the relative lower fold changes in *Tert* in HSPCs compared with total bone marrow may also be due to higher levels of endogenous *Tert* in HPSCs compared with whole bone marrow. As a control, AAV9-*Tert* treatment of wild-type mice did not affect the relative numbers of lineage-positive or -negative cells or the proportion of HSPCs (supplemental Figure 2). Given the increased *Tert* expression in HSPCs, we next addressed whether this affected their proliferation/colony-forming potential. To this end, we performed a colony-forming cell assay (MethoCult). We observed a significantly increased number of colonies in the bone marrow from AAV9-*Tert*-treated mice compared with those treated with the empty vector (Figure 1H).

In summary, IV injection of AAV9 vectors administered at a high dose can target *Tert* to hematopoietic cells, including HSPCs.

### AAV9-*Tert* treatment rescues survival in a mouse model of aplastic anemia

We next tested whether treatment with AAV9-*Tert* was effective in increasing survival upon induction of lethal aplastic anemia due to critically short telomeres. First, we used the conditional *Trf1* mouse model recently developed by us (*Trf1<sup>lox/lox</sup> Mx1-Cre* mice) in which we induce partial *Trf1* deletion specifically in the bone marrow.<sup>19</sup> To this end, we transplanted lethally irradiated wild-type mice with bone marrow isolated from *Trf1<sup>lox/lox</sup> Mx1-Cre* mice, followed by administration of pI:pC to induce the expression of Cre recombinase and *Trf1* deletion.<sup>19,20</sup> Genotyping confirmed that the new bone marrow solely consisted of donor cells with excisable *Trf1* (supplemental Figure 3). Thus, *Trf1<sup>lox/lox</sup> Mx1-Cre* mice allow study of the effects of *Trf1* depletion exclusively in the bone marrow. We previously showed that partial *Trf1* deletion in the bone marrow results in rapid death and removal of the *Trf1*-deleted cells, whereas cells that fail to delete *Trf1* undergo compensatory rounds of cell division, leading to rapid telomere shortening and replicative senescence, eventually resulting in bone marrow failure.<sup>19,20</sup>

Here, we induced *Trf1* deletion with pI:pC injections at a frequency of 3 times per week for 5 weeks, at which point these mice started to show signs of aplastic anemia.<sup>19,20</sup> One week after the last pI:pC injection, mice were treated with either the AAV9-*Tert* or AAV9-empty vector (Figure 2A). Mouse survival was monitored for 100 days after treatment with the AAV9 vectors (note: beyond 100 days after virus treatment, none of the mouse cohorts developed signs of aplastic anemia. At 120 days post-virus administration, all mice were euthanized for further analyses). Strikingly, AAV9-*Tert* treatment significantly increased survival: 87% of mice were still alive at 100 days after virus administration in the AAV9-*Tert*-treated group compared

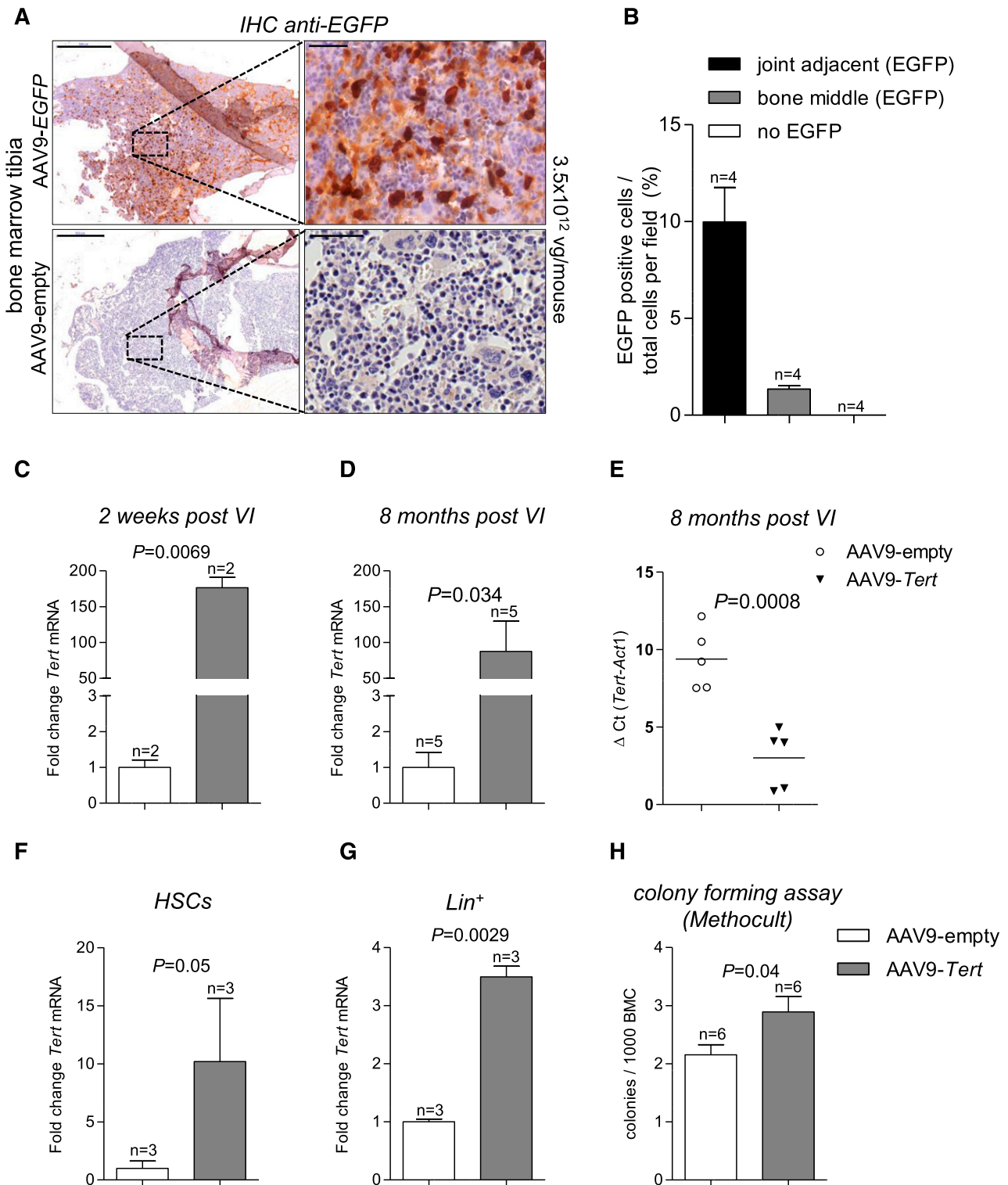


**Figure 1. High dose of AAV9 particles targets bone marrow, including HSPCs.** (A) Representative anti-EGFP immunohistochemistry (IHC) images of bone marrow corresponding to the tibia. Mice were injected with the AAV9-EGFP vector or AAV9-empty vector at a concentration of  $3.5 \times 10^{12}$  viral genomes (vg) per mouse. EGFP-positive cells were mainly located toward the end of the bones. Bars represent 500  $\mu$ m (left) and 50  $\mu$ m (right); hematoxylin and eosin stain. (B) Percentage of EGFP-positive cells relative to the total number of cells. Cells were separately counted in joint adjacent areas and in the middle of the bone. (C-D) *Tert* mRNA expression level in total bone marrow isolated 2 weeks (C) and 8 months (D) after VI with  $3.5 \times 10^{12}$  viral genomes per mouse. AAV9-*Tert* relative to the expression of mice injected with the same amount of AAV9-empty vector. (E)  $\Delta$  Ct values (*Tert* minus *Act1*) of the quantitative real-time PCR shown in panel D. Quantitative real-time PCR determined relative *Tert* expression in HSPCs (HSCs) sorted by FACS (F) and lineage-committed cells (G). (H) Colony-forming assay in MethoCult with whole bone marrow cells isolated from mice injected with AAV9-*Tert* or AAV9-empty. For all experiments, n indicates number of mice. Data are mean  $\pm$  SEM. Statistical analysis: 2-sided Student *t* test; *P* values are shown. SEM, standard error of the mean; VI, virus injection.

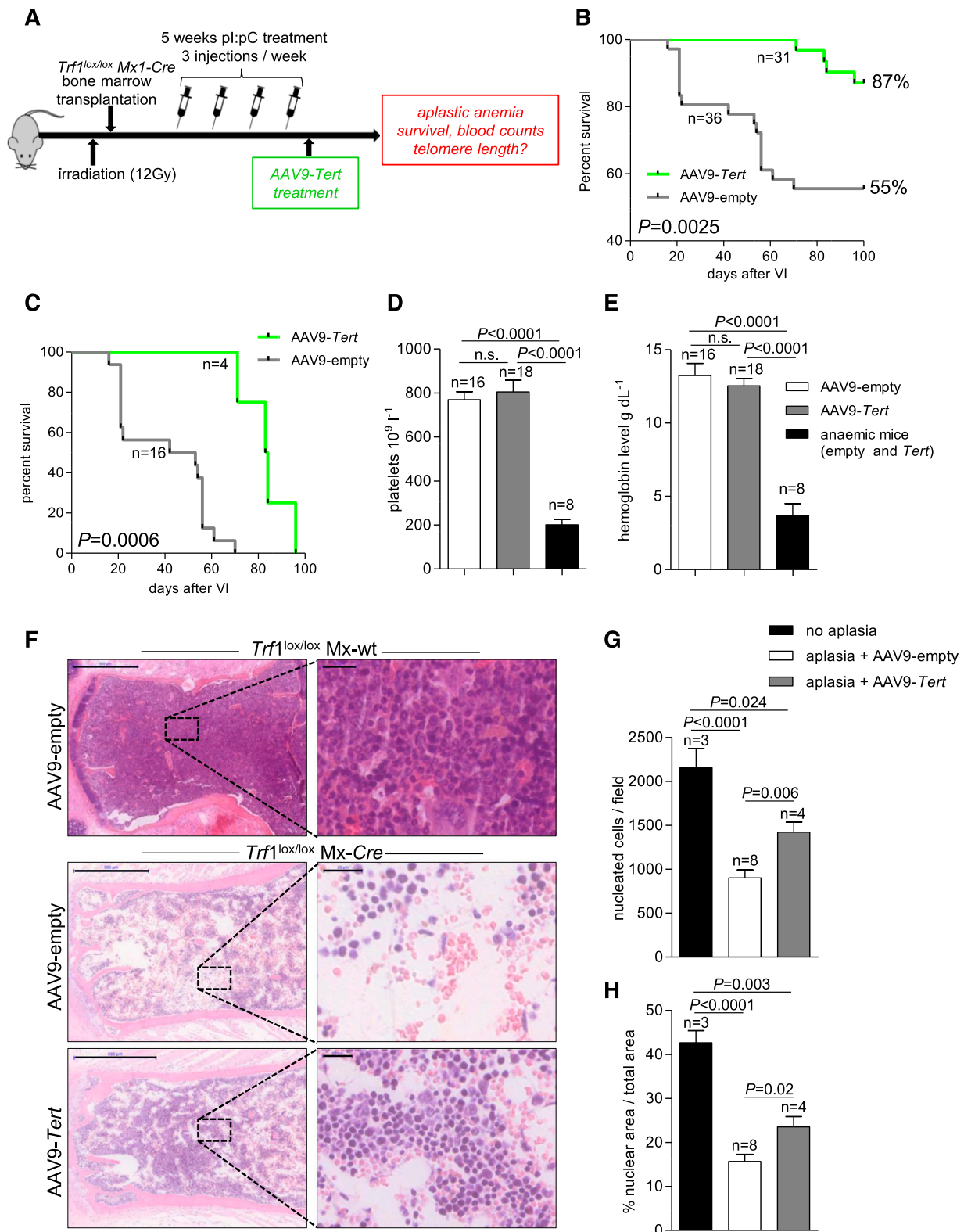


**Figure 2. AAV9-Tert treatment rescues the aplastic anemia phenotype in *Trf1*<sup>lox/lox</sup> mice.** (A) Experimental design. Mice were lethally irradiated and transplanted the following day with *Trf1*<sup>lox/lox</sup> *Mx1-Cre* bone marrow. After engraftment, *Cre* expression and *Trf1* excision was induced by pl:pC injections for 5 weeks. One week later, mice were injected with AAV9-Tert or AAV9-empty particles. (B) Kaplan-Meier survival curves showing that AAV9-Tert treatment significantly rescues mouse survival. (C) Kaplan-Meier survival curves considering only those animals that died of aplastic anemia within 100 days after virus treatment show significant protection of AAV9-Tert treatment from deaths due to aplastic anemia. Platelet counts (D) and hemoglobin levels (E) in mice of the AAV9-Tert-treated and AAV9-empty-treated groups showing clear signs of anemia compared with healthy mice from the same AAV9-Tert-treated and AAV9-empty-treated groups. (F) Representative bone marrow images of healthy controls (no *Cre*-mediated induction of *Trf1* deletion) and of mice with bone marrow aplasia. Genotypes and AAV9 treatments are indicated. Bars represent 500  $\mu$ m (left) and 20  $\mu$ m (right); hematoxylin and eosin stain. (G) Quantification of bone marrow cellularity expressed as number of nucleated cells per field. Four to 5 fields per mouse were counted. (H) Quantification of bone marrow cellularity expressed as the percentage of nuclear area (purple stain) to total areas per field. Four to 5 fields per mouse were counted. In all graphs, n indicates number of mice. Data are mean  $\pm$  SEM. Statistical analysis: log-rank test in panels B and C; 2-sided Student *t* test in panels D, E, G, and H; *P* values are shown. n.s., not significant.

with only 55% of mice alive in the empty vector–treated group (Figure 2B). In particular, whereas only 4 of 31 mice (13%) treated with AAV9-*Tert* developed aplastic anemia, 16 of 36 mice (44%) died with clear signs of aplastic anemia in the group treated with the empty vector (Figure 2C). In both groups, aplastic anemia was determined as the cause of death in those mice showing a drastic drop in platelet counts and hemoglobin levels at the time of death (Figure 2D-E) and presenting with severe bone marrow hypoplasia and aplasia after postmortem histopathological analysis of bone marrow sections (Figure 2F). Interestingly, among those mice that died of aplastic anemia, we observed a tendency to show a milder bone marrow aplasia phenotype in the AAV9-*Tert*-treated group compared with the AAV9-empty-treated group, as indicated by higher bone marrow cellularity in the AAV9-*Tert*-treated group (Figure 2F). Quantification of the bone marrow cellularity confirmed a drastic decrease of cellularity in aplastic anemia mice compared with wild-type control mice. Of importance, the decrease in cellularity was significantly attenuated in the AAV9-*Tert*-treated cohort compared with the AAV9-empty-treated group (Figure 2G-H). Our results suggest that AAV9-*Tert* treatment of mice with induced severe telomere shortening significantly reduces mortality due to aplastic anemia.

#### Telomerase treatment reverses telomere shortening in peripheral blood and bone marrow cells in a mouse model of aplastic anemia

Because aplastic anemia in our mouse model is caused by extreme telomere shortening,<sup>19,20</sup> we next compared the dynamics of telomere length in mice treated with AAV9-*Tert* vs mice treated with the empty vector. To this end, we performed a longitudinal study to follow telomere length in peripheral blood (PBMCs) over time using telomere HT-Q-FISH technology.<sup>34</sup> To do so, we extracted blood at 4 different time points (time point 1, 30 days after bone marrow engraftment; time point 2, 5 weeks after pI:pC treatment; time point 3, 2 months after treatment with the AAV9 vectors; and time point 4, 4 months after treatment with the AAV9 vectors) (note: longitudinal telomere measurements were done on PBMCs from mice that did not develop aplastic anemia). In agreement with previous findings, we found a dramatic drop in telomere length of ~10 kb in all mice after induction of *Trf1* deletion with pI:pC and prior to treatment with the gene therapy vectors (Figure 3A; compare time points 1 and 2).<sup>19,20</sup> We observed a further drop in telomere length in those mice treated with the AAV9-empty vector when comparing time point 4 with time point 2 in this mouse cohort (Figure 3A-B). Importantly, during the same period of time, mice treated with AAV9-*Tert* showed a net increase in average telomere length of 10 kb when comparing time point 4 with time point 2 (Figure 3A-B). Indeed, throughout the course of the experiment, AAV9-empty-treated mice showed a total decrease in average telomere length of 12 kb, whereas mice treated with AAV9-*Tert* showed re-elongation of telomeres to a similar telomere length as before the induction of *Trf1* deletion by pI:pC treatment (Figure 3C). These findings indicate that AAV9-*Tert* treatment is sufficient to stop and even revert initial telomere shortening. To further confirm whether telomeres were elongated as the consequence of AAV9-*Tert* gene therapy specifically in the bone marrow, we performed Q-FISH analysis on bone marrow cross-sections at the end point of the experiment. In agreement with longer telomeres in peripheral blood cells in the AAV9-*Tert*-treated mice, we found that AAV9-*Tert*-treated mice also had significantly longer telomeres in the bone marrow compared with mice treated with the empty vector (Figure 3D-F). We confirmed the AAV9-*Tert*-mediated telomere elongation on independent samples using a real-time PCR

assay for relative telomere length determination<sup>30,31</sup> (supplemental Figure 4A). Furthermore, in line with our hypothesis that aplastic anemia is the consequence of drastically shortened telomeres, mice treated with the AAV9-empty vector that developed aplastic anemia had significantly shorter telomeres than mice that were treated in the same manner but did not develop aplastic anemia (supplemental Figure 4B).

Of note, telomere length analysis on bone marrow sections or bone marrow DNA does not allow one to distinguish between various cell populations. However, the observed telomere elongation in PBMCs suggests a direct effect of AAV9-*Tert* on HSPCs.

#### Telomerase gene therapy of aplastic anemia produced by short telomeres resulting from *Tert* deletion improves blood counts and increases telomere length

To validate the therapeutic use of telomerase gene therapy in aplastic anemia provoked by short telomeres, we used an additional mouse model for modeling short telomere length in the hematopoietic system (in this case due to telomerase deficiency during several mouse generations): the *Tert*-deficient mouse model.<sup>22</sup> To this end, we irradiated wild-type mice and transplanted them with bone marrow from G3 *Tert*-knockout mice, which have short telomeres in all mouse tissues, including the bone marrow<sup>22</sup> (Figure 4A). First, we confirmed shorter telomeres in the G1 and G3 *Tert*-knockout bone marrow donors compared with the wild-type bone marrow donors by performing HT-Q-FISH analysis on PBMCs. In particular, *Tert* deficiency leads to progressive telomere shortening, with G3 mice having an average telomere length of ~25 kb compared with ~40 kb in the wild-type controls (Figure 4B). One month after transplantation of irradiated wild-type mice with G3 *Tert* knockout bone marrow, mice were divided in 2 groups and treated with either AAV9-*Tert* or AAV9-empty gene therapy vectors ( $3.5 \times 10^{12}$  viral genomes per mouse) (Figure 4A). After treatment, we monitored mice during a follow-up period of 5 months and observed robust expression of *Tert* in the bone marrow in the AAV9-*Tert*-treated group (supplemental Figure 5). Importantly, in response to AAV9-*Tert* treatment, we observed an increase in survival compared with the AAV9-empty-treated group that almost reached statistical significance ( $P = .058$ ) (Figure 4C). Upon mouse euthanasia, *Tert*-treated mice had significantly increased hemoglobin levels and higher erythrocyte and platelet counts compared with mice treated with the empty vector (Figure 4D-F). The same trend was observed for leukocyte counts, which were higher in AAV9-*Tert*-treated mice compared with the AAV9-empty group, although the trend did not reach statistical significance ( $P = .09$ ) (Figure 4G). Lastly, to analyze the mechanism by which *Tert* gene therapy improved survival and blood counts in these mice, we followed longitudinally the telomere length in PBMCs in both mouse cohorts. To this end, we extracted blood before and 3 and 5 months after mice were injected with the viruses and performed HT-Q-FISH analysis. In line with the results obtained with the *Trf1*<sup>lox/lox</sup> mouse model (see “AAV9-*Tert* treatment rescues survival in a mouse model of aplastic anemia”), we found that AAV9-*Tert* treatment led to a net increase in average telomere length of 5.18 kb with time, whereas during the same period, mice treated with the AAV9-empty vector suffered a slight telomere shortening of -1.76 kb (Figure 5A-B). These findings were also confirmed by telomere Q-FISH analysis on bone marrow sections at 5 months after virus administration. In particular, we found significantly longer telomeres in the bone marrow of *Tert*-treated mice compared with mice treated with the empty vector (Figure 5C-D).

In summary, these results indicate that a single treatment with the AAV9-*Tert* vector in mice with previously shortened telomeres in the bone marrow due to telomerase deficiency is sufficient to increase

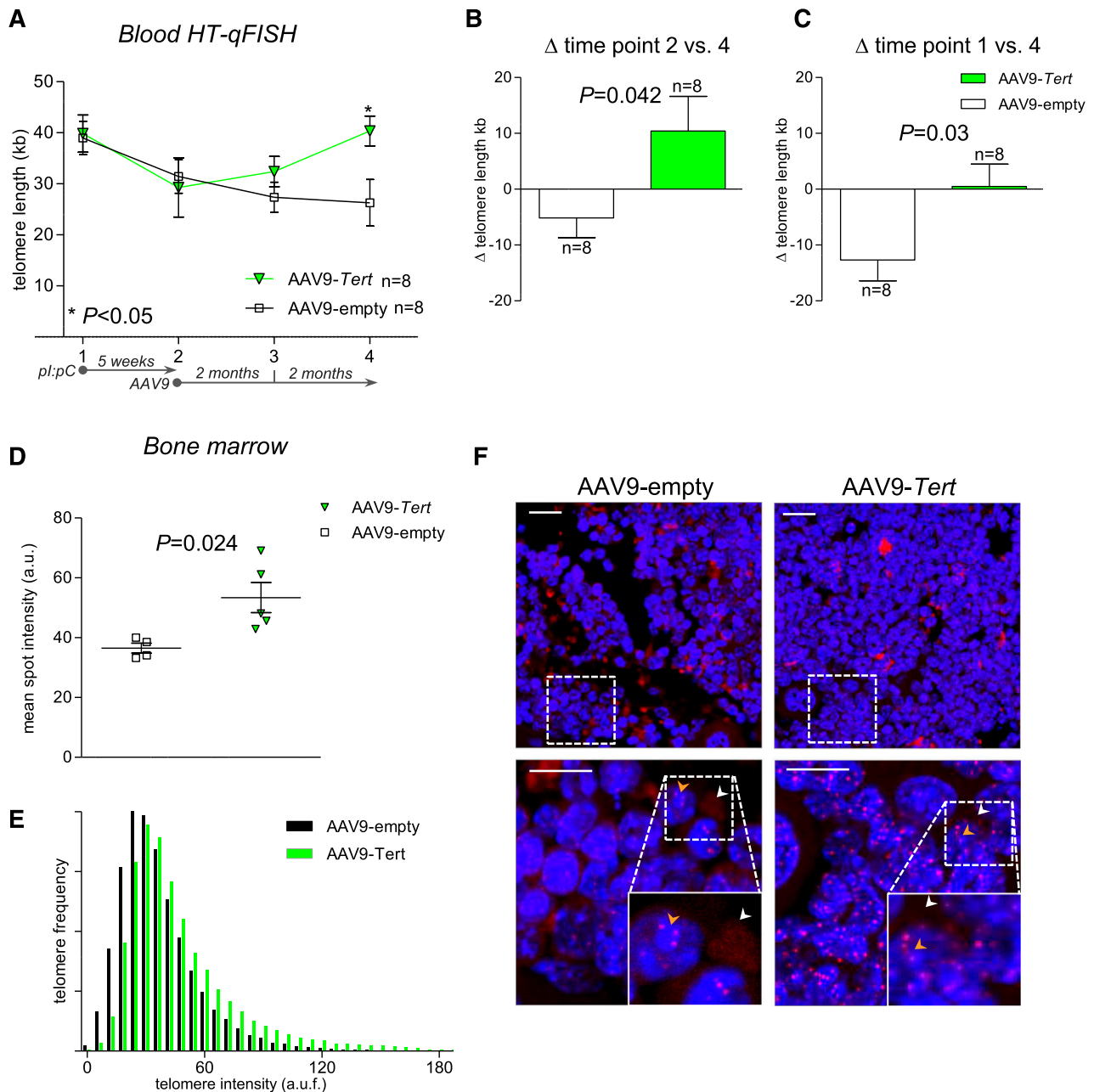


**Figure 3. AAV9-Tert treatment causes telomere elongation in blood and bone marrow.** (A) Longitudinal HT-Q-FISH analysis of telomere length in peripheral blood monocytes (*Tf1<sup>lox/lox</sup> Mx1-Cre*-transplanted mice; see also Figure 2A). Blood was extracted at 4 different time points (time point 1, before pl:pC treatment; time point 2, after 5 weeks of pl:pC treatment and before AAV9 injection; time point 3, 2 months after AAV9 injection; and time point 4, 4 months after AAV9 injection). Relative variation ( $\Delta$ ) of telomere length in AAV9-Tert-treated and AAV9-empty-treated animals between time points 2 and 4 (B) and between time points 1 and 4 (C). (D) Relative telomere length in bone marrow sections from AAV9-Tert-treated and AAV9-empty-treated mice shown as arbitrary units of fluorescence (a.u.f.). Each square and triangle represents the mean telomere length per nucleus of an individual mouse. (E) Frequency distribution blot of telomere length showing a higher abundance of short telomeres in the AAV9-empty-treated group compared with AAV9-Tert-treated mice (pooled data from panel D). (F) Representative images of bone marrow sections from AAV9-Tert-treated and AAV9-empty-treated mice used for Q-FISH analysis. Cell nuclei are stained blue (DAPI) and telomeres are stained red (Cy3). White arrowheads indicate nonspecific extranuclear signals and yellow arrowheads indicate specific telomere signals within DAPI-stained nuclei. Bars represent 20  $\mu\text{m}$  (top) and 10  $\mu\text{m}$  (bottom). In all graphs, n indicates number of mice. Data are mean  $\pm$  SEM. Statistical analysis: 2-way analysis of variance in panel A; 2-sided Student *t* test in panels B and C; *P* values are shown. a.u., arbitrary units.

telomere length in the bone marrow and in blood. Telomerase gene therapy also improved blood counts and mouse survival.

## Discussion

Here, we set out to test the hypothesis of whether increased expression of telomerase through systemic virus-based *Tert* delivery may delay or

prevent the emergence of aplastic anemia provoked by short telomeres. We tested this hypothesis in 2 independent mouse models with very short telomeres specifically in the bone marrow due to either *Tf1* or *Tert* deficiency.<sup>20,22</sup>

The rationale for this study was based on our previous finding showing that systemic AAV9-Tert gene therapy in wild-type mice was sufficient to delay different age-related diseases and to significantly increase mouse life span by delaying telomere shortening with age in different tissues.<sup>18</sup> A 5-month longitudinal follow-up of these mice also

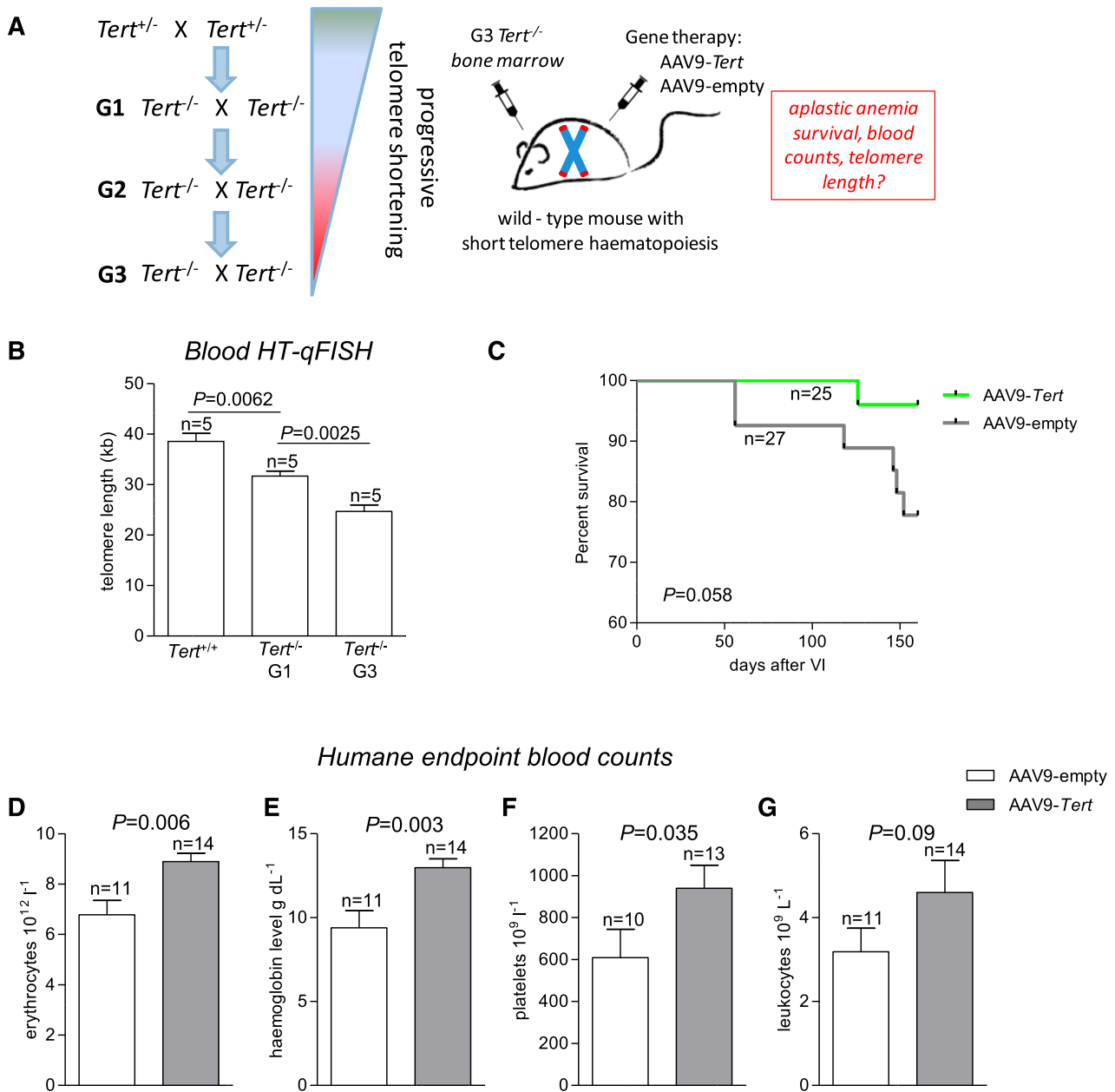


**Figure 4. AAV9-Tert treatment improves blood counts in mice with short telomeres resulting from specific *Tert* deletion in the bone marrow.** (A) Experimental design. G3  $Tert^{-/-}$  mice with short telomeres were generated by consecutive crosses of *Tert*-deficient mice. Bone marrow from these G3 mice was isolated and transplanted into irradiated wild-type mice. After engraftment, mice were injected with AAV9-Tert or AAV9-empty virus particles. (B) HT-Q-FISH analysis of telomere length in PBMCs from wild-type, G1  $Tert^{-/-}$ , and G3  $Tert^{-/-}$  mice reveals progressive telomere shortening with consecutive mouse generations. (C) Kaplan-Meier survival curves show that AAV9-Tert treatment improves survival of mice with very short telomeres in the bone marrow due to *Tert* deficiency specifically in the bone marrow (irradiated wild-type mice transplanted with G3  $Tert^{-/-}$  bone marrow). AAV9-Tert compared with AAV9-empty treatment improves erythrocyte counts (D), hemoglobin levels (E), platelet counts (F), and leukocyte counts (G). In all graphs, n indicates number of mice. Data are mean  $\pm$  SEM. Statistical analysis: log-rank test in panel A; 2-sided Student *t* test in panels B and E-H; *P* values are shown.

revealed increased telomere length in PBMCs from mice treated with telomerase gene therapy, suggesting that the vectors were also targeting the bone marrow.<sup>18</sup> This finding is in line with recent reports showing that AAV9 viral genome copies are readily detectable in bone marrow isolates even 20 weeks postinjection<sup>35</sup> and with the fact that FACS analysis of bone marrow from neonatal mice administered AAV9-green fluorescent protein show increased amounts of green fluorescent protein-positive cells.<sup>36</sup> Thus, *Tert* delivery via AAV9 may hold potential for treating aplastic anemia triggered or associated with short telomeres in the bone marrow, a common consequence of telomerase

mutations in the so-called telomeropathies or telomere syndromes, as well as in some acquired cases of aplastic anemia.<sup>37-39</sup>

To demonstrate this, we first confirmed that a high dose ( $3.5 \times 10^{12}$  viral genomes per mouse) of AAV9-EGFP reporter vector injected IV was able to transduce the bone marrow, as indicated by the presence of EGFP-positive cells. Furthermore, administration of the same amount of AAV9-Tert particles led to robust *Tert* expression in whole bone marrow isolates 2 weeks after treatment; this increased expression was maintained at 8 months posttreatment. To rule out the possibility that AAV9 may be targeting only bone marrow stroma cells, we

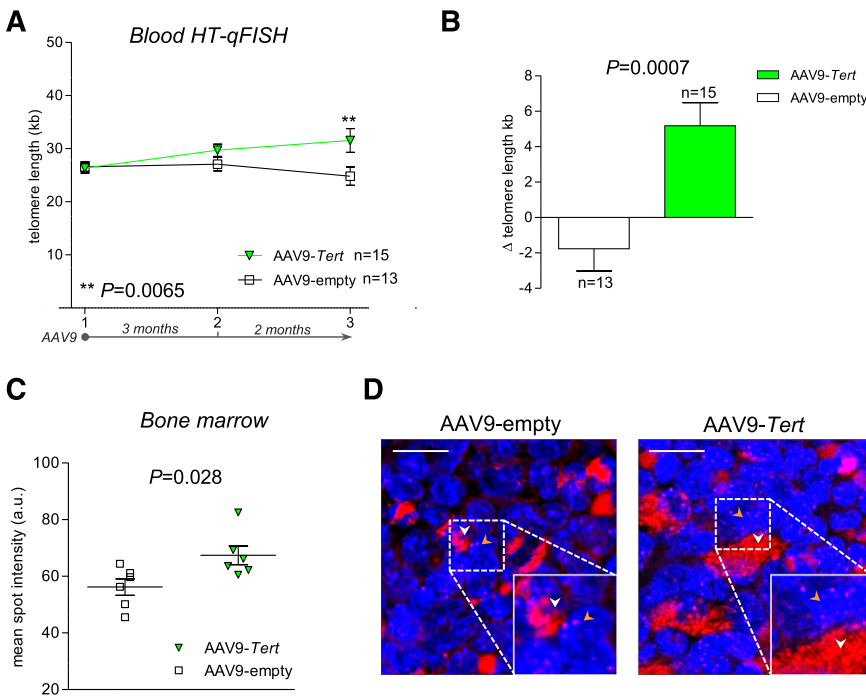


**Figure 5. Telomerase gene therapy leads to telomere elongation in peripheral blood and bone marrow cells from mice with specific deletion of *Tert* in the bone marrow.** (A) Longitudinal HT-Q-FISH analysis of telomere length in PBMCs of irradiated wild-type mice transplanted with bone marrow from G3 *Tert*<sup>-/-</sup> mice (see also Figure 4A). Blood was extracted at 3 different time points (time point 1, after G3 *Tert*<sup>-/-</sup> bone marrow engraftment and before AAV9 injection; time point 2, 3 months after AAV9 injection; and time point 3, 5 months after AAV9 injection). (B) Relative variation (Δ) of telomere length in AAV9-*Tert*-treated and AAV9-empty-treated animals between time points 1 and 3. (C) Telomere Q-FISH analysis on bone marrow sections from animals transplanted with G3 *Tert*<sup>-/-</sup> bone marrow and treated with AAV9-empty or AAV9-*Tert* for 5 months before euthanasia. Each square or triangle represents the mean telomere length per nucleus (expressed as arbitrary units of fluorescence) of an individual mouse. (D) Representative images of bone marrow sections from AAV9-*Tert*-treated and AAV9-empty-treated mice used for Q-FISH analysis. Cell nuclei are stained blue (DAPI) and telomeres are stained red (Cy3). White arrowheads indicate nonspecific extranuclear signals and yellow arrowheads indicate specific telomere signals within DAPI-stained nuclei. Bars represent 10 μm. For all experiments, n indicates number of mice. Data are mean ± SEM. Statistical analysis: 2-way analysis of variance in panel A; 2-sided Student *t* test in panels B and C; *P* values are shown.

demonstrated significantly increased *Tert* mRNA expression both in isolated hematopoietic stem cells (*lin*<sup>-</sup>, *Sca-1*<sup>+</sup>, *c-kit*<sup>+</sup>) and in lineage-committed bone marrow cells (*lin*<sup>+</sup>) from mice treated with AAV9-*Tert* compared with mice treated with the AAV9-empty vector. Importantly, bone marrow cells from AAV9-*Tert*-treated mice showed enhanced colony-forming abilities, suggesting that telomerase expression may increase the stem cell reserve.

Indeed, AAV9-*Tert* treatment of mice with aplastic anemia triggered by short telomeres resulting from marrow-specific *Tf1* deletion<sup>19</sup> significantly rescued mortality due to aplastic anemia, concomitant with telomere re-elongation in blood and bone marrow cells from these mice after telomerase treatment. We confirmed these findings by generating a second mouse model of aplastic anemia produced by short telomeres, in this case due to telomerase deficiency. In particular, we generated mice with *Tert* deficiency specifically in the bone marrow. In this case, the treatment of *Tert* gene therapy in mice with *Tert*-deficient bone marrow and short telomeres (irradiated wild-type mice transplanted with G3 *Tert*-knockout bone marrow) showed a moderate improvement of survival, which was not as dramatic as in the case of the *Tf1*-deficient bone marrow model. This result is likely due to the fact that in contrast to the *Tf1*-deletion model, which shows a very severe and rapid induction of aplastic anemia,<sup>19,20</sup> *Tert* deficiency leads to a variable penetrance of aplastic anemia with increasing mouse generations.<sup>40,41</sup> Similarly to the *Tf1*-deficient mouse model, *Tert* gene therapy of the *Tert*-deficient bone marrow mouse model also resulted in increased telomere length with time in peripheral blood cells and significantly improved blood counts. In both mouse models, improvement of blood counts can be interpreted as the consequence of improved stem cell reserve. This is in line with recently published data showing that genetic *Tert* re-activation in fifth-generation *Tert*<sup>-/-</sup> mice using a Cre-inducible system restored HSPC proliferation, concomitant with improved erythrocyte counts and hemoglobin levels.<sup>42</sup>

In summary, we provide proof of concept for a therapeutic effect of telomerase treatment using AAV9 gene therapy vectors in the treatment of aplastic anemia provoked by short telomeres. A strategy based on AAV9-*Tert* treatment may be beneficial not only in the correction of

monogenic bone marrow disease such as in carriers of *Tert* mutations (we demonstrated improved blood counts in *Tert*-knockout mice) but also in other forms of aplastic anemia associated with short telomeres and hematopoietic stem cell depletion (eg, Fanconi anemia<sup>43</sup>). Generally, due to an excellent safety profile attributable to their low immunogenicity and the fact that they are nonintegrative, AAV vectors have become an attractive gene therapy tool, and many clinical trials using those vectors are already underway (see [www.clinicaltrials.gov](http://www.clinicaltrials.gov)). However, despite the fact that AAV9 vectors carrying the *Tert* gene are nonintegrative and therefore unlikely to aid in the division of cancer cells, the association of many cancers with telomerase expression imposes specific safety concerns. In this regard, it is important to point out that in a previous study, a longer than 1-year follow-up of wild-type mice treated with AAV9-*Tert* did not show increased cancer; in fact, cancer onset was delayed in the same manner as other age-related diseases.<sup>18</sup> Nevertheless, subsequent studies should address the safety of this strategy in long-lived mammals such as primates. If those studies confirm our proof-of-principle findings, this gene therapy approach may also be adapted to treat hereditary forms of aplastic anemia caused by mutations other than *Tert* by replacing the gene to be delivered.

## Acknowledgments

This study was funded by the Spanish Ministry of Economy and Competitiveness, the Fundación Botín, and the Roche Extending the Innovation Network Academia Partnering Program (M.A.B.).

## Authorship

Contribution: M.A.B. conceived the original idea; M.A.B. and C.B. designed the experiments and wrote the paper; C.B. performed the majority of the experiments; R.S. performed the bone marrow

transplants and monitored the mice during all animal procedures; J.M.P., M.P., and C.B.-B. performed the experiments during the revision process; I.F. and M.B. contributed to scientific discussions and the experimental design; and F.B. provided the viral vectors.

Conflict-of-interest disclosure: The authors declare no competing financial interests.

The current affiliation for C.B. is Institute of Molecular and Translational Therapeutic Strategies, Hannover Medical School, Hannover, Germany.

Correspondence: Maria A. Blasco, Spanish National Cancer Research Center, Melchor Fernández Almagro 3, Madrid E-28029, Spain; e-mail: mblasco@cni.es.

## References

- Scopes J, Bagnara M, Gordon-Smith EC, Ball SE, Gibson FM. Haemopoietic progenitor cells are reduced in aplastic anaemia. *Br J Haematol*. 1994;86(2):427-430.
- Maciejewski JP, Anderson S, Katevas P, Young NS. Phenotypic and functional analysis of bone marrow progenitor cell compartment in bone marrow failure. *Br J Haematol*. 1994;87(2):227-234.
- Marsh JC, Ball SE, Cavenagh J, et al; British Committee for Standards in Haematology. Guidelines for the diagnosis and management of aplastic anaemia. *Br J Haematol*. 2009;147(1):43-70.
- Nakao S. Immune mechanism of aplastic anemia. *Int J Hematol*. 1997;66(2):127-134.
- Dokal I, Vulliamy T. Inherited bone marrow failure syndromes. *Haematologica*. 2010;95(8):1236-1240.
- Brümmendorf TH, Maciejewski JP, Mak J, Young NS, Lansdorp PM. Telomere length in leukocyte subpopulations of patients with aplastic anemia. *Blood*. 2001;97(4):895-900.
- Blackburn EH. Switching and signaling at the telomere. *Cell*. 2001;106(6):661-673.
- de Lange T. Shelterin: the protein complex that shapes and safeguards human telomeres. *Genes Dev*. 2005;19(18):2100-2110.
- Harley CB, Futcher AB, Greider CW. Telomeres shorten during ageing of human fibroblasts. *Nature*. 1990;345(6274):458-460.
- Flores I, Canela A, Vera E, Tejera A, Cotsarelis G, Blasco MA. The longest telomeres: a general signature of adult stem cell compartments. *Genes Dev*. 2008;22(5):654-667.
- Hiyama E, Hiyama K. Telomere and telomerase in stem cells. *Br J Cancer*. 2007;96(7):1020-1024.
- Wynn RF, Cross MA, Hatton C, et al. Accelerated telomere shortening in young recipients of allogeneic bone-marrow transplants. *Lancet*. 1998;351(9097):178-181.
- Ball SE, Gibson FM, Rizzo S, Tooze JA, Marsh JC, Gordon-Smith EC. Progressive telomere shortening in aplastic anemia. *Blood*. 1998;91(10):3582-3592.
- Flores I, Cayuela ML, Blasco MA. Effects of telomerase and telomere length on epidermal stem cell behavior. *Science*. 2005;309(5738):1253-1256.
- Vulliamy T, Marrone A, Dokal I, Mason PJ. Association between aplastic anaemia and mutations in telomerase RNA. *Lancet*. 2002;359(9324):2168-2170.
- Dokal I. Dyskeratosis congenita. *Hematology Am Soc Hematol Educ Program*. 2011;2011:480-486.
- Tummala H, Walne A, Collopy L, et al. Poly(A)-specific ribonuclease deficiency impacts telomere biology and causes dyskeratosis congenita. *J Clin Invest*. 2015;125(5):2151-2160.
- Bernardes de Jesus B, Vera E, Schneeberger K, et al. Telomerase gene therapy in adult and old mice delays aging and increases longevity without increasing cancer. *EMBO Mol Med*. 2012;4(8):691-704.
- Beier F, Foronda M, Martinez P, Blasco MA. Conditional TRF1 knockout in the hematopoietic compartment leads to bone marrow failure and recapitulates clinical features of dyskeratosis congenita. *Blood*. 2012;120(15):2990-3000.
- Bär C, Huber N, Beier F, Blasco MA. Therapeutic effect of androgen therapy in a mouse model of aplastic anemia produced by short telomeres. *Haematologica*. 2015;100(10):1267-1274.
- Martínez P, Thanasoula M, Muñoz P, et al. Increased telomere fragility and fusions resulting from TRF1 deficiency lead to degenerative pathologies and increased cancer in mice. *Genes Dev*. 2009;23(17):2060-2075.
- Liu Y, Snow BE, Hande MP, et al. The telomerase reverse transcriptase is limiting and necessary for telomerase function in vivo. *Curr Biol*. 2000;10(22):1459-1462.
- Samper E, Fernández P, Eguía R, et al. Long-term repopulating ability of telomerase-deficient murine hematopoietic stem cells. *Blood*. 2002;99(8):2767-2775.
- Matsushita T, Elliger S, Elliger C, et al. Adeno-associated virus vectors can be efficiently produced without helper virus. *Gene Ther*. 1998;5(7):938-945.
- Ayuso E, Mingozzi F, Montane J, et al. High AAV vector purity results in serotype- and tissue-independent enhancement of transduction efficiency. *Gene Ther*. 2010;17(4):503-510.
- Ayuso E, Blouin V, Lock M, et al. Manufacturing and characterization of a recombinant adeno-associated virus type 8 reference standard material. *Hum Gene Ther*. 2014;25(11):977-987.
- Samper E, Goytisolo FA, Slijepcevic P, van Buul PP, Blasco MA. Mammalian Ku86 protein prevents telomeric fusions independently of the length of TTAGGG repeats and the G-strand overhang. *EMBO Rep*. 2000;1(3):244-252.
- Canela A, Klatt P, Blasco MA. Telomere length analysis. *Methods Mol Biol*. 2007;371:45-72.
- McIlrath J, Bouffler SD, Samper E, et al. Telomere length abnormalities in mammalian radiosensitive cells. *Cancer Res*. 2001;61(3):912-915.
- Cawthon RM. Telomere measurement by quantitative PCR. *Nucleic Acids Res*. 2002;30(10):e47.
- Callicott RJ, Womack JE. Real-time PCR assay for measurement of mouse telomeres. *Comp Med*. 2006;56(1):17-22.
- Inagaki K, Fuess S, Storm TA, et al. Robust systemic transduction with AAV9 vectors in mice: efficient global cardiac gene transfer superior to that of AAV8. *Mol Ther*. 2006;14(1):45-53.
- Jimenez V, Muñoz S, Casana E, et al. In vivo adeno-associated viral vector-mediated genetic engineering of white and brown adipose tissue in adult mice. *Diabetes*. 2013;62(12):4012-4022.
- Canela A, Vera E, Klatt P, Blasco MA. High-throughput telomere length quantification by FISH and its application to human population studies. *Proc Natl Acad Sci USA*. 2007;104(13):5300-5305.
- Huang J, Li X, Coelho-dos-Reis JG, Wilson JM, Tsuji M. An AAV vector-mediated gene delivery approach facilitates reconstitution of functional human CD8<sup>+</sup> T cells in mice. *PLoS One*. 2014;9(2):e88205.
- Mattar CN, Wong AM, Hoefer K, et al. Systemic gene delivery following intravenous administration of AAV9 to fetal and neonatal mice and late-gestation nonhuman primates. *FASEB J*. 2015;29(9):3876-3888.
- Armanios M, Blackburn EH. The telomere syndromes. *Nat Rev Genet*. 2012;13(10):693-704.
- Calado RT, Young NS. Telomere diseases. *N Engl J Med*. 2009;361(24):2353-2365.
- Kirwan M, Dokal I. Dyskeratosis congenita, stem cells and telomeres. *Biochim Biophys Acta*. 2009;1792(4):371-379.
- Herrera E, Samper E, Blasco MA. Telomere shortening in mTR<sup>-/-</sup> embryos is associated with failure to close the neural tube. *EMBO J*. 1999;18(5):1172-1181.
- Herrera E, Samper E, Martín-Caballero J, Flores JM, Lee HW, Blasco MA. Disease states associated with telomerase deficiency appear earlier in mice with short telomeres. *EMBO J*. 1999;18(11):2950-2960.
- Raval A, Behbehani GK, Nguyen XT, et al. Reversibility of defective hematopoiesis caused by telomere shortening in telomerase knockout mice. *PLoS One*. 2015;10(7):e0131722.
- Dokal I, Vulliamy T. Inherited aplastic anaemias/ bone marrow failure syndromes. *Blood Rev*. 2008;22(3):141-153.



- Her insan DNA düzeyinde eşsizdir. Anti-aging tedavi de DNA düzeyinde kişiye özel olmalıdır.
- Bireylerin genetik olarak yaşlanma eğilimlerini belirleyen testtir.

- CİLT**
- 1 Sıklık + Esneklik Kabiliyeti
  - 2 UV Dayanıklılığı + Pigmentasyon
- TÜM VÜCUT**
- 3 Glikasyon Direnci (A.G.E.)
  - 4 Serbest Radikal Direnci
  - 5 Hassasiyet + İnflamasyona Yatkınlık

- Kritik düzeyde kısalmış telomerlerin boyunu ve miktarını ölçen genetik testtir.
- Test biyolojik yaş tespiti için kullanılır. Yıllık ölçümler yaparak yaşlanma hızı belirlenip, yönetilebilir.

# TA65®

www.tasciences.com



## TA-65 MD® 250 Ünite, 90 kapsül

- Astragalus bitkisinden elde edilen özel bir molekül ile formüle edilmiş besin desteğidir.
- Yemeklerden 2-3 saat sonra günde 1 kapsül alınması önerilir.
- Uzun süreli kullanımı güvenli olup, düzenli alınması önerilir.



## TA-65 for Skin 30 ml - 118 ml

- Anti-aging amaçlı cilt bakım kremidir.
- Patentli TA-65® etken maddesi içerir.
- Temiz cilde günde 2 kez uygulanır.
- Tüm yaş ve cilt tiplerine uygundur.
- Paraben içermez.
- Airless tüp içinde kullanıma sunulur.
- Dermatolojik olarak test edilmiştir.

Satın almak için;